IDENTIFICATION OF LINEAR STRUCTURAL MODELS

by

Nelson Glenn Creamer

Dissertation submitted to the Faculty of the
Virginia Polytechnic Institute and State University
in partial fulfillment of the requirements for the degree of
DOCTOR OF PHILOSOPHY
in
Engineering Science and Mechanics

APPROVED:

Dr. J.L./Junkins

Dr. W.L. Hallauer

Dr. S.L. Hendricks

Dr. J.N. Reddy

Dr. D.P. Telionis

March, 1987

Blacksburg, Virginia

IDENTIFICATION OF LINEAR STRUCTURAL MODELS

by

Nelson Glenn Creamer

(ABSTRACT)

With a great amount of research currently being aimed towards dynamic analysis and control of very large, flexible structures, the need for accurate knowledge of the properties of a structure in terms of the mass, damping, and stiffness matrices is of extreme importance. Typical problems associated with existing structural model identification methods are: (i) non-unique solutions may be obtained when utilizing only free-response measurements (unless some parameters are fixed at their nominal values), (ii) convergence may be difficult to achieve if the initial estimate of the parameters is not "close" to the truth, (iii) physically unrealistic coupling in the system matrices may occur as a consequence of the identification process, (iv) large, highly redundant parameter sets may be required to characterize the system, and (v) large measurement sets may be required. To overcome these problems, a novel identification technique is developed in this dissertation to determine the mass, damping, and stiffness matrices of an undamped, lightly damped, or significantly damped structure from a small set of measurements of both free-response data (natural frequencies, damping factors) and forced-response data (frequency response functions).

The identification method is first developed for undamped structures. Through use of the spectral decomposition of the frequency

response matrix and the orthogonality properties of the mode shapes, a unique identification of the mass and stiffness matrices is obtained. The method is also shown to be easily incorporated into a substructure synthesis package for identifying high-order systems. The method is then extended to include viscous damped structures. A matrix perturbation approach is developed for lightly damped structures, in which the mass and stiffness matrices are identified using the imaginary components of the measured eigenvalues and, as a post-processor, the damping matrix is obtained from the real components of the measured eigenvalues. For significantly damped structures, the mass, damping, and stiffness matrices are identified simultaneously.

A simple, practical method is also developed for identification of the time-varying relaxation modulus associated with a viscoelastic structure. By assuming time-localized elastic behavior, the relaxation modulus is determined from a series of identification tests performed at various times throughout the response history.

Many interesting examples are presented throughout the dissertation to illustrate the applicability and potential of the identification method. It is observed from the numerical results that the uniquely identified structure agrees with simulated measurements of both free- and forced-response records.

ACKNOWLEDGEMENTS

I would like to express my deepest gratitude to my friend and advisor, Dr. John L. Junkins, for providing invaluable assistance in the form of helpful suggestions, motivation, and financial support. The highly productive, yet pleasingly informal work environment provided by Dr. Junkins has made life as a graduate student almost enjoyable, and the time spent under his leadership will surely be considered the "turning point" in my professional career.

I would also like to extend my sincere appreciation to Dr. W.L. Hallauer, Dr. S.L. Hendricks, Dr. J.N. Reddy, and Dr. D.P. Telionis for the time they spent serving as members of the committee.

Finally, I would like to thank for the many hours of excellent help she provided in the typing and overall editing of the dissertation.

TABLE OF CONTENTS

LIST OF FIGURES

LIST OF TABLES

1. INTRODUCTION

A parametric (or mathematical) model of a continuous structure represents a discrete mathematical description of the structure in configuration space, consisting of the classical mass, damping, and stiffness matrices. The determination of these matrices requires a discretization process via (in most cases) the highly-developed finite element method. Although the finite element analysis of a structure can yield very accurate results, the method is only as accurate as the values of the parameters described in the element equations (i.e. EI, EA, ρ, etc.) . The accurate knowledge of the parameters of the structural model becomes extremely important when considering the many proposed large, highly flexible space structures for which the response characteristics may be quite sensitive to initial "model ignorance." Accurate knowledge of the parameters is also of fundamental importance when designing active control schemes for vibration suppression and attitude maneuvering. In addition, variations in the parameters of a structure can occur due to environmental exposure, viscoelastic processes, and material degradation. It therefore becomes very important for the structural dynamicist to address and explore the following fundamental question: "What modifications should be made to an existing mathematical model in the event that the theoretical results do not agree with corresponding experimental results?" In the following chapters, the search for the answer(s) to this question begins with a survey of existing techniques (along with their corresponding advantages and disadvantages), proceeds with the development of a novel method

applicable to both undamped (or lightly damped) and damped systems, and concludes with interesting numerical examples which demonstrate the flexibility and potential of the method. Before embarking on this journey, however, it is necessary to distinguish between two general categories of parameter estimation methods.

1.1 Modal Model Identification Vs. Structural Model Identification

The branch of structural dynamics which addresses the problem of estimating a set of parameters from measured response records is called *system identification*. The field of system identification consists of two general categories: modal model identification (MMI) and structural model identification (SMI). Under the category of modal model identification, which involves the determination of the system natural frequencies, damping factors, and mode shapes, there are generally two classes of methods. Frequency-domain methods consist of single-degree-of-freedom and multi-degree-of-freedom curve fits of the frequency response function throughout the frequency domain of interest. On the other hand, time-domain methods consist of curve fitting forced and/or unforced time-domain records to obtain state-space realizations from which the modal properties can be obtained.

In contrast to modal model identification, the determination of the mass, damping, and stiffness matrices (or parameterizations thereof) is referred to as structural model identification. Many SMI methods utilize measured eigenvalue and eigenvector data, therefore requiring MMI as a pre-processor. The technique developed in this dissertation

represents a novel SMI method, the outline of which is discussed in the following section.

1.2 Organization of the Dissertation

The dissertation begins in Chapter 2 with a literature survey of existing SMI methods in terms of both common parameterization schemes utilized and corresponding identification techniques. Advantages and disadvantages of each method are discussed in detail.

Because of their importance as pre-processors for SMI methods, a brief review of frequency- and time-domain MMI methods is presented in the first section of Chapter 3. The Ibrahim Time Domain method and the Eigensystem Realization Algorithm are developed in detail. In the second section, a novel SMI method is developed for linear elastic, undamped structures utilizing measured natural frequencies and frequency response functions. Incorporation of the identification method into a broadly useful substructure synthesis technique is then developed. Interesting examples are used to study the potential of the method. Extension of the SMI method for application to linear elastic, viscous damped structures is developed in the third section, in which two techniques are established: a state-space approach for structures exhibiting general viscous damping, and a configuration-space perturbation approach for structures exhibiting light viscous damping. Again, example applications demonstrate the potential and flexibility of the method.

Identification of linear viscoelastic structures is addressed in

Chapter 4. Some common analysis methods are first reviewed and then a simple, practical approach to the estimation of the relaxation modulus is developed by assuming time-localized elastic properties. An example is used to demonstrate the approach.

Finally, some concluding remarks are presented in Chapter 5, as well as a discussion of potential areas for further research.

2. A SURVEY OF STRUCTURAL MODEL IDENTIFICATION METHODS

Parametric structural identification is a rich and highly-researched field with a wide variety of existing techniques. A survey is complicated by the diversity of approaches and by the differing extent to which various approaches have been brought to analytical and practical maturity. Before proceeding with a discussion of some commonly used methods, it is worthwhile to mention some of the previous reviews on this subject. Astrom and Eykhoff [1] and Bekey [2] present surveys of system identification techniques through 1970. Techniques of model parameter estimation are reviewed for both linear and nonlinear models. Ibanez [3] provides a review of experimental procedures and parameter identification methods in both the time and frequency domain through 1978 and summarizes a number of earlier reviews. Sage [4] classifies and summarizes identification methods under three branches: (i) transfer function identification, (ii) learning model identification, and (iii) nonlinear filtering. Collins, Young, and Kiefling [5] present technology trees in both the time and frequency domain and classify identification methods in terms of direct and iterative approaches. Hart and Yao [6] provide updated versions of the technology trees and review identification methods under three categories: (i) no prior structural model available, (ii) an approximate model available with no modeling or experimental error quantification, and (iii) an approximate model available along with error quantification. Berman [7] and Berman and Flannelly [8] present reviews of identification methods by classifying the methods into three

areas: (i) direct verification of an existing model, (ii) direct modification of an existing model, and (iii) direct identification of a structural model.

In the first section of this chapter a brief description of the more common parameterization methods is presented. In the second section, an overview of a variety of identification methods developed for each parameterization scheme is presented as well as the advantages and disadvantages of each.

2.1 Parameterization Methods

An efficient review of the various methods available for identifying a structural model of a system begins with a categorization of the parameterization schemes most commonly used. Each category leads to a parameter set which must be identified (estimated) in order that the corresponding response of the structural model be brought into best agreement with the corresponding measured response. The type of parameters used to characterize the model plays a central role in determining which identification method is most suitable.

The most common and generally applicable method of modeling a flexible structure is the finite element method [43]. The consequences of this discretization procedure are the well-known global mass and stiffness matrices, which are functions of a set of specified parameters. The parameter set consists of physical properties associated with the structure (i.e. densities, Young's moduli, cross-sectional areas, lengths, discrete masses, etc.) [13-27], and is

obviously dependent upon the discretization scheme (type of finite elements selected, etc.). Every finite element may have its own set of parameters so that the total size of this physical parameter set can be quite large for complex structures.

Many space structures, although large in size and complex in detail, behave grossly as a beam, plate, or shell. In view of this fact, an interesting method of parameterization is one in which the structure is treated as an equivalent simple continuum model, leading to a set of equivalent continuum parameters [28-32]. The attractiveness of this approach is not only that the finite element model is greatly simplified but also that the size of the equivalent parameter set is potentially much smaller than the finite element set of physical parameters. This approach is most attractive for beam-like and plate-like lattice structures with repeating patterns and has proven to be quite accurate in predicting natural frequencies and mode shapes associated with the macroscopic deformations of these structures.

In some identification techniques the parameter set does not necessarily correspond to physical properties inherent in a model of the structure. These techniques can be separated into two general classes: those which utilize an initial, approximate model of the structure (through finite element analysis, for example) and those which are independent of any modeling process. One method of parameterization, which requires the availability of an initial finite element model, is to update the global mass and stiffness matrices by adding (assembling) scaled versions of prescribed submatrices in such a way as to improve the accuracy of the global model [33]. These submatrices can represent

a single finite element or, more commonly, groups of elements having assumed identical or similar geometry, material properties, boundary conditions, and modeling assumptions. This parameter set, which consists of the submatrix scale factors, will be used in the structural model identification method developed in Chapter 3. Another "non-physical" parameterization technique simply estimates small (minimum Euclidian norm) modifications for both the mass and stiffness matrices, with the parameter set consisting of the elements of the modification matrices [34-38].

The parameterization methods listed above require the availability of an initial approximate model of the structure, therefore coupling the identification and modeling processes. However, if there is little or no reliable information available for the structure (which would be the worst possible scenario) then there is no modeling process to rely upon and, if a conventional discrete linear model is desired, it becomes necessary to identify all elements of the mass, damping, and stiffness matrices [39-42]. In the sequel, methods for identifying these various parameter sets will be reviewed.

2.2 Identification of Parametric Structural Models

In the previous section various parameterization methods (commonly used in conjunction with identification) were reviewed. Some of the more popular identification techniques will now be reviewed and compared in more detail to establish the relative merits of each. Consider first those methods which identify the fundamental physical/geometrical

properties of the structure directly. The major advantages of these methods are that the actual physical properties of the structural model are identified and, in the process, the internal consistency of the finite element model (or any other discretized representation) is maintained. The major disadvantage stems from the fact that the structural responses (natural frequencies, mode shapes, displacements, etc.) are generally nonlinear functions of the parameters, therefore requiring iterative procedures in which convergence is dependent upon the degree of nonlinearity and the accuracy of the starting estimates. Obviously, a secondary disadvantage arises if the actual physics of the structure are not captured with sufficient precision by the modeling approach taken. There are two identification (estimation) methods which are most commonly used: the least-squares (or weighted least-squares) method [9] and the Bayesian method [10-11]. The Bayesian approach can be viewed as a weighted least-squares method with the incorporation of a priori parameter estimates. A tutorial on the relationship between the least-squares method, the Bayesian method, and other similar methods is provided by Isenberg [12].

Hendricks, et. al. [13] and Creamer and Hendricks [14] use the least-squares method to identify the physical parameters of a simple planar structure consisting of a rigid hub and four flexible appendages. Using a Jacobian matrix, containing eigenvalue sensitivities with respect to the various parameters, Hendricks identifies a relatively small set of parameters from a larger set of measured eigenvalues (natural frequencies and damping factors). It is shown that the parameters can be accurately identified as long as a

characteristic mass, length, and time scale are provided (which is accomplished most directly by fixing some selected parameters at their nominal values) and the initial estimate of the parameters is "close" to the truth. Alternatively, a priori estimates of the selected parameters can be introduced, as in Bayesian estimation and similar approaches. Knowledge of the characteristic scales is required because the measurements of the eigenvalues are obtained from the free-vibration (unforced) response of the structure. Caravani, et. al. [15] use a recursive least-squares algorithm to identify the mass and stiffness parameters of a simple two degree-of-freedom system from time-domain measurements. Chen and Garba [16] utilize an approach in which a few very accurate measurements of natural frequencies are used to identify a larger set of parameters. A minimum-norm iterative method is used to select the one solution (out of an infinite number of possibilities) which yields the smallest changes in the values of the estimated parameters. In applying this method to the Viking Orbiter propulsion system, it is shown that the final identified model can be highly dependent upon the measurements available and the selection of the subset of parameters used to update the model.

The Bayesian estimation method is a statistical method for updating a set of parameters by utilizing prescribed confidence levels associated with the initial values of the parameters. Many applications of the Bayesian estimator can be found in the literature. One of the first applications is given by Collins et. al. [17] who identify a set of bending and shear rigidity parameters for the Saturn-Apollo launch vehicle from measurements of natural frequencies and mode shapes. Dobbs

and Nelson [18] use natural frequency measurements to determine mass and stiffness parameters for an offshore platform. To reduce the numerical effort associated with the estimator, Dobbs incorporates a "parameter linking" constraint procedure in which certain parameters are held in fixed proportion to one another. Beliveau [19] uses measurements of natural frequencies, damping factors, mode shapes, and phase angles to identify viscous damping parameters for a general framework. Hasselman and Johnson [20] and Fries and Cooperrider [21] use the Bayesian estimator to validate and verify a structural model and its parameters for rail-vehicle systems. Fries and Cooperrider utilize frequency response measurements in place of eigenvalue/eigenvector measurements so that the Jacobian matrix represents frequency response sensitivities to the various parameters of interest. Other similar applications of the Bayesian estimator are given in References [22] through [24].

Hasselman [25] postulates a set of bounds for evaluating the quality of the Bayesian estimated parameters in terms of their associated increase in confidence levels. For visual inspection of the qualification of the estimate, a "significance" plot is presented by Hasselman for incorporating the bounds in graphical form. Hasselman further observes that correct use of the Bayesian estimator requires (i) realistic estimates of the measurement uncertainty, (ii) realistic estimates of the initial parameter uncertainty, and (iii) use of measurements that are sufficiently sensitive to the parameters being estimated.

Hart and Martinez [26] use an Iterated Extended Kalman Filter algorithm to identify a set of physical parameters using frequency

response data. In a recent paper, Martinez [27] reviews and examines the estimation of a set of parameters via least-squares and statistical (Bayesian) methods and their relation to the more general Extended Kalman Filter algorithm.

The large parameter sets associated with high degree of freedom, complex structures may require computationally expensive identification efforts, regardless of the method employed. However, many large space structures can be treated grossly as a beam, plate, or shell, or a simple assembly thereof. These equivalent continuum models usually contain far fewer parameters than the higher order discrete models and therefore are quite attractive for some identification purposes. Noor and Anderson [28], Chen and Sun [29], and Sun et. al. [30] develop methods for obtaining the equivalent continuum parameters for lattice structures.

The least-squares estimator or the Bayesian estimator can be used to identify the parameters of equivalent continuum models. Juang and Sun [31] and Sun and Juang [32] address the problem of identifying the equivalent continuum parameters of a lattice structure by minimizing a quadratic error cost function, in terms of differences in theoretical and experimental impulse responses, with a random search algorithm. It should be noted that the same disadvantages that occur when attempting to identify actual physical parameters are also present when the parameter set consists of equivalent continuum parameters; that is, an iterative procedure is required in which convergence is dependent upon the degree of nonlinearity, the accuracy of the initial estimates, and the observability of the estimated parameters.

In the identification methods discussed to this point, the parameter set consists of physical properties of the structure such as mass density, modulus of elasticity, and bending rigidity. The remaining identification methods to be discussed utilize parameter sets consisting of matrix scaling factors or the matrix elements themselves to fit available experimental results. The first methods to be reviewed are those requiring an initial approximate model of the structure. White and Maytum [33] identify a set of matrix scaling factors which, when multiplied by prescribed submatrices, improve the accuracy of the global model. The submatrices can represent a single finite element or a group of finite elements having the same assumed geometry, material properties, boundary conditions, and modeling assumptions. White utilizes an energy matrix, representing the modal kinetic and potential energy distributions of each submatrix, to obtain a least-squares estimate of the scale factors such that modeled natural frequencies agree with their measured counterparts. This energy matrix is also utilized in the structural model identification method developed in Chapter 3. The main disadvantage with the White/Maytum method is that either part of the mass matrix or part of the stiffness matrix must be held fixed at its nominal value because only free-response measurements are utilized (to provide appropriate scaling of the equations requires forced-response data). In the example they present, the complete mass matrix is fixed at its nominal value.

In another approach, which also utilizes an initial approximate model of the structure, Berman and Flannely [34] and Berman and Nagy [35] improve initial mass and stiffness matrices by adding small

modifications determined from a set of measured natural frequencies and mode shapes. In updating the model, the eigenvalue equation and the orthonormality conditions of the mode shapes are enforced as equality constraints for minimizing error functions for the corrections added to the mass matrix [36] and the stiffness matrix [37]. The advantages of this method are (i) the computational procedure is simple and requires no iterative process and (ii) the improved model predicts the measured natural frequencies and mode shapes exactly. The disadvantages are (i) use solely of measured free-vibration responses does not provide a unique solution, (ii) the final mass and stiffness matrices often do not resemble the correct mass and stiffness matrices and, in fact, physically unrealistic coupling often occurs, and (iii) both natural frequency and mode shape measurements are required.

In an approach similar to Berman's method, Chen et. al. [38] utilize matrix perturbation theory to improve initial mass and stiffness matrices. The perturbation matrices are determined from the orthonormality conditions on the mode shapes. The same disadvantages occur in this method that are present in Berman's method. A key point worth noting is that identification of a damped structure is not addressed in White's method, Berman's method, or Chen's method.

If there is no approximate mathematical model available for the structure, or if the model is deemed unsatisfactory, a recovery of effective mass and stiffness matrix elements can be sought directly from measurements. A method developed by Potter and Richardson [39] utilizes an identified set of modal normalization factors, obtained from the spectral decomposition of the frequency response matrix, along with

measurements of natural frequencies, damping factors, and mode shapes to identify the mass, damping, and stiffness matrices. However, in their formulation, measurements of all of the eigenvalues and eigenvectors of the structure are required, a luxury which would be highly unlikely in most real applications.

Rajaram [40], Rajaram and Junkins [41], and Hendricks et. al. [42] use a set of forced response measurements of displacements, velocities, and accelerations to uniquely determine the elements of the mass, damping, and stiffness matrices. The order of the system, and therefore the maximum size of the uniquely determined parameter set, is established by the number of measurement locations prescribed during the data gathering phase of the identification process. The advantages of this method are (i) due to the utilization of forced response data, a uniquely identified parameter set is obtained and (ii) all parameters appear linearly in the equations of motion, therefore requiring no iterative procedure and no initial estimate. The disadvantages are (i) a large set of measurements (and spatially dense measurement locations) is usually required, (ii) the parameter set is large and highly redundant for most applications since there are often many more elements in the mass, damping, and stiffness matrices than the required number of fundamental physical parameters, and (iii) knowledge of sparsity which might be present in the matrices is not utilized.

It becomes evident from the literature survey that a variety of methods exist for identifying the structural model of a system, with each method exhibiting disadvantages which could prove unacceptable for a given application. In the following chapters, a computationally

efficient method is developed which uniquely identifies the mass, damping, and stiffness matrices of a structure from a limited set of free- and forced-vibration measurements without the need for "fixing" any parameters at their original values and without the imposition of any physically unrealistic coupling as a consequence of the identification process.

3. IDENTIFICATION OF LINEAR ELASTIC STRUCTURES

In this chapter a novel structural model identification method is developed for improving the mass, damping, and stiffness matrices of an initial finite element model such that the theoretical predictions of the frequency response matrix and the system eigenvalues and eigenvectors agree with corresponding experimental results. In the second and third sections the method is outlined for identifying undamped and damped structural models, respectively, from experimental measurements. However, because of their importance in the formulation and implementation of the identification method, the chapter begins with a brief overview of frequency- and time-domain methods for obtaining measurements of frequency response functions and modal parameters.

3.1 Modal Model Identification

Identification of the modal parameters of a structure (natural frequencies, damping factors, mode shapes) has received much attention over the past twenty years. As the demand for accurate and precise dynamic measurements of complex structures increased, early methods of simple "deduction by observation" of dynamic response in both the time domain and the frequency domain became obsolete. With the advent of the Fast-Fourier-Transform (FFT) spectrum analyzers in the early 70's came the possibility of a very fast means of determining the experimental output-to-input ratio in the form of the frequency response function (FRF). In parallel with the frequency-domain methods, modal

identification directly from time-response records received greater attention with the introduction of the Ibrahim Time Domain (ITD) method in the mid 70's and, most recently, the Eigensystem Realization Algorithm (ERA) in the mid 80's. In the sequel, the frequency-domain and time-domain methods will be reviewed in more detail.

3.1.a Frequency-Domain Methods

The backbone of the frequency-domain methods of modal parameter extraction is the determination of the frequency response function [44] defined as the ratio of the output to input,

$$H(\omega) = \frac{X(\omega)}{F(\omega)} \tag{3.1}$$

where $X(\omega)$ and $F(\omega)$ are the Fourier-transformed output and input, respectively. However, since both the input and output records can contain extraneous noise from external sources and/or nonlinearities, frequency response measurements are not usually determined according to Eq.(3.1). Defining the auto-spectra of the input and output as

$$G_{ff}(\omega) = F^{*}(\omega)\, F(\omega) \tag{3.2a}$$

$$G_{xx}(\omega) = X^{*}(\omega)\, X(\omega) \tag{3.2b}$$

and the cross-spectra between the input and output as

$$G_{fx}(\omega) = F^{*}(\omega)\, X(\omega) \tag{3.3a}$$

$$G_{xf}(\omega) = X^{*}(\omega)\, F(\omega) \tag{3.3b}$$

where the asterisk denotes the complex conjugate operation, two revised forms of the frequency response function become [45-49]

$$H_1(\omega) = \frac{G_{fx}(\omega)}{G_{ff}(\omega)} \tag{3.4a}$$

$$H_2(\omega) = \frac{G_{xx}(\omega)}{G_{xf}(\omega)} \tag{3.4b}$$

Taking the ensemble averages of the auto-spectra and cross-spectra over many different time records diminishes the effects of undesirable random noise so that use of Eqs.(3.4a) or (3.4b) represent a better approximation to the true frequency response function then Eq.(3.1). Equation (3.4b) is preferred near resonant conditions because of the high response signal-to-noise ratio in these regions. Equation (3.4a) is preferred near antiresonant conditions because of the low response signal-to-noise ratio in these regions [48,49]. A qualitative assessment of the accuracy of the frequency response function can be obtained from the coherence function, defined as

$$\gamma^2 = \frac{H_1(\omega)}{H_2(\omega)} = \frac{|G_{xf}(\omega)|^2}{G_{xx}(\omega)\, G_{ff}(\omega)} \qquad 0 \le \gamma \le 1 \tag{3.5}$$

A coherence of 1 represents perfectly consistent estimates from Eqs.(3.4) and any value less than 1 indicates noise-corrupted results.

After obtaining the frequency response function the task now becomes extraction of the modal parameters of each measured mode. There exists several single-degree-of-freedom and multi-degree-of-freedom techniques for extracting these parameters [44]. The single-degree-of-freedom methods assume that behavior of a system in the vicinity of resonance is dominated by a single mode (an assumption that is inaccurate for closely-spaced or repeated modes). These methods utilize least-squares circle fits of the Nyquist plots, along with the spectral decomposition of the FRF (see Equations (3.32) and (3.83)), in the local vicinity of each mode to extract the natural frequencies, damping factors, and modal constants. The multi-degree-of-freedom methods involve curve-fitting the entire frequency response function over the frequency range of interest for the structure using the spectral decomposition of the FRF in this region [50-53].

3.1.b Time-Domain Methods

The two most widely-used time-domain modal identification methods are the Ibrahim Time Domain method [54-56] and the Eigensystem Realization Algorithm [57-59]. The Ibrahim Time Domain method utilizes free-response measurements of a structure at different time intervals to determine the modal parameters. Assuming a response at time t_1 of the form

$$x(t_1) = x_1 = \sum_{j=1}^{2n} p_j e^{\lambda_j t_1} \tag{3.6}$$

where x and p are the n-dimensional response vector and eigenvector, respectively, the response at 2n different times can be written as

$$[x_1\ x_2\ \cdots\ x_{2n}] = [p_1\ p_2\ \cdots\ p_{2n}]\begin{bmatrix} e^{\lambda_1 t_1} & e^{\lambda_1 t_2} & \cdots & e^{\lambda_1 t_{2n}} \\ e^{\lambda_2 t_1} & & \ddots & e^{\lambda_2 t_{2n}} \\ \vdots & & & \\ e^{\lambda_{2n} t_1} & & \cdots & e^{\lambda_{2n} t_{2n}} \end{bmatrix} \tag{3.7a}$$

or $$X = P\,\Lambda \tag{3.7b}$$

Responses at time Δt later become

$$[y_1\ y_2\ \cdots\ y_{2n}] = [q_1\ q_2\ \cdots\ q_{2n}]\,\Lambda \tag{3.8a}$$

or $$Y = Q\,\Lambda \tag{3.8b}$$

where $$q_i = p_i e^{\lambda_i \Delta t} \tag{3.8c}$$

Similarly, responses occuring at time $2\Delta t$ later become

$$[z_1\ z_2\ \cdots\ z_{2n}] = [r_1\ r_2\ \cdots\ r_{2n}]\,\Lambda \tag{3.9a}$$

or $$Z = R\,\Lambda \tag{3.9b}$$

where $$r_i = q_i e^{\lambda_i \Delta t} = p_i e^{2\lambda_i \Delta t} \tag{3.9c}$$

Grouping Eqs.(3.7b) and (3.8b) together yields

$$\begin{bmatrix} X \\ Y \end{bmatrix} = \begin{bmatrix} P \\ Q \end{bmatrix} \Lambda \tag{3.10a}$$

or $$\phi = \psi \Lambda \tag{3.10b}$$

Grouping Eqs.(3.8b) and (3.9b) together yields

$$\begin{bmatrix} Y \\ Z \end{bmatrix} = \begin{bmatrix} Q \\ R \end{bmatrix} \Lambda \tag{3.11a}$$

or $$\hat{\phi} = \hat{\psi} \Lambda \tag{3.11b}$$

Eliminating Λ from Eqs.(3.10b) and (3.11b) and using Eqs.(3.8c) and (3.9c) results in the eigenvalue problem

$$\hat{\phi}\, \phi^{-1} \psi_i = e^{\lambda_i \Delta t} \psi_i \tag{3.12}$$

Solving the eigenvalue problem of Eq.(3.12) leads to the complex eigenvalues and eigenvectors of the system.

The Eigensystem Realization Algorithm begins with the equations of motion in the discrete state-space form

$$x(k+1) = Ax(k) + Bu(k) \tag{3.13a}$$

$$y(k) = Cx(k) \qquad k=0,1,2,... \tag{3.13b}$$

where A is the n x n state matrix, B is the n x m input influence matrix, and C is the ℓ x n output influence matrix. The ***Markov parameters*** are defined as the ℓ x m impulse response matrices

$$Y(1)=CB,\ Y(2)=CAB,\ \ldots,\ Y(k)=CA^{k-1}B,\ \ldots \tag{3.14}$$

obtained by assembling the m impulse responses, at each time $t_k=k\Delta t$, defined by the inputs

$$u(0) = \text{col}\{0,0,\ldots,u_i=1,0,0,\ldots\} \quad i=1,2,\ldots,m \tag{3.15a}$$

$$u(k) = \text{col}\{0,0,\ldots\} \quad k=1,2,\ldots \tag{3.15b}$$

$$x(0) = \text{col}\{0,0,\ldots\} \tag{3.15c}$$

The Markov parameters can be recovered from measured transfer functions or from impulse response measurements. Next the $(r+1)\ell \times (s+1)m$ block *Hankel matrix* is formed

$$H(k-1) = \begin{bmatrix} Y(k) & Y(k+1) & \ldots & Y(k+s) \\ Y(k+1) & & & \\ \vdots & & & \vdots \\ Y(k+r) & & \ldots & Y(k+s+r) \end{bmatrix} \tag{3.16}$$

It can be verified by direct expansion that the Hankel matrix can be factored into the form

$$H(k-1) = \begin{bmatrix} C \\ CA \\ \vdots \\ CA^r \end{bmatrix} A^{k-1} \begin{bmatrix} B & AB & \ldots & A^sB \end{bmatrix} \tag{3.17a}$$

$$= V_r A^{k-1} W_s \tag{3.17b}$$

where V_r is the $(r+1)\ell \times n$ *observability* matrix and W_s is the $n \times (s+1)m$ *controllability* matrix. Defining the $\ell \times (r+1)\ell$ matrix $E_\ell = [I_\ell \; 0_\ell \; 0_\ell \; \ldots]$ and the $(s+1)m \times m$ matrix $E_m = [I_m \; 0_m \; 0_m \; \ldots]$, the Markov parameter $Y(k)$ can be written as

$$Y(k) = E_\ell H(k-1) \; E_m \tag{3.18a}$$

$$= E_\ell V_r A^{k-1} W_s E_m \tag{3.18b}$$

Now defining the $(s+1)m \times (r+1)\ell$ matrix H^+ as

$$W_s H^+ V_r = I_n \tag{3.19}$$

yields the result

$$Y(k) = E_\ell V_r [W_s H^+ V_r] \; A^{k-1} [W_s H^+ V_r] \; W_s E_m \tag{3.20}$$

Note that the matrix H^+ represents a general pseudo-inverse of $H(0)$ from

$$V_r W_s H^+ V_r W_s = V_r W_s = H(0) \tag{3.21a}$$

or $$H(0) \; H^+ H(0) = H(0) \tag{3.21b}$$

The matrix H(0) can be factored using Singular Value Decomposition [60] to obtain

$$H(0) = P \begin{bmatrix} D_r & 0 \\ 0 & 0 \end{bmatrix} Q^T = [P_r \; P_{rest}] \begin{bmatrix} D_r & 0 \\ 0 & 0 \end{bmatrix} \begin{Bmatrix} Q_r^T \\ Q_{rest}^T \end{Bmatrix} \tag{3.22a}$$

$$= P_r D_r Q_r^T \tag{3.22b}$$

where the columns of P and Q are orthonormal and D_r (= diag[d_1, d_2, ..., d_r]) contains the singular values. Solving for H^+ using Eqs.(3.21b) and (3.22b) yields

$$H^+ = Q_r D_r^{-1} P_r^T \tag{3.23}$$

Substituting Eq.(3.23) into (3.20) gives

$$Y(k) = E_\ell V_r W_s Q_r D_r^{-1} P_r^T V_r A^{k-1} W_s Q_r D_r^{-1} P_r^T V_r W_s E_m \tag{3.24a}$$

$$= E_\ell H(0) \; Q_r D_r^{-1} P_r^T V_r A^{k-1} W_s Q_r D_r^{-1} P_r^T H(0) \; E_m \tag{3.24b}$$

$$= E_\ell H(0) \; Q_r D_r^{-\frac{1}{2}} [D_r^{-\frac{1}{2}} P_r^T V_r A^{k-1} W_s Q_r D_r^{-\frac{1}{2}}] \; D_r^{-\frac{1}{2}} P_r^T H(0) \; E_m \tag{3.24c}$$

$$= E_\ell H(0) \; Q_r D_r^{-\frac{1}{2}} [D_r^{-\frac{1}{2}} P_r^T H(1) \; Q_r D_r^{-\frac{1}{2}}]^{\,k-1} \; D_r^{-\frac{1}{2}} P_r^T H(0) \; E_m \tag{3.24d}$$

$$= E_\ell P_r D_r^{\frac{1}{2}} [D_r^{-\frac{1}{2}} P_r^T H(1) \; Q_r D_r^{-\frac{1}{2}}]^{\,k-1} \; D_r^{\frac{1}{2}} Q_r^T E_m \tag{3.24e}$$

Comparing Eqs.(3.24e) and (3.14) gives the *minimum realization*

$$\hat{A} = D_r^{-\frac{1}{2}} P_r^T H(1)\, Q_r D_r^{-\frac{1}{2}} , \quad \hat{B} = D_r^{\frac{1}{2}} Q_r^T E_m , \quad \hat{C} = E_\ell P_r D_r^{\frac{1}{2}} \tag{3.25}$$

The complex system eigenvalues and eigenvectors can now be determined from the eigenvalues and eigenvectors of $\hat{A}$.

3.2 Structural Model Identification of Undamped Structures

In the previous section identification of the modal model of a structure using input-output measurements was reviewed in both the frequency domain and the time domain. It was also shown that the Eigensystem Realization Algorithm not only identifies the modal parameters of a structure but also determines a best-fitting discrete "non-parametric" time-domain model in state space. Although this is a powerful and widely applicable method, the fundamental disadvantages of this approach are i) the absence of initial mathematical modeling assumptions (i.e. through finite element discretizations) leads to increased dimensionality of the estimation process and ii) the method does not provide structural engineers with direct insight to refine their highly-developed finite element model and its consequences in the form of the improved mass and stiffness matrices.

In this section the results from the modal identification process are used to develop a structural model identification method applicable to undamped structures. In the first subsection the identification method is introduced and developed; in the second subsection the method

is integrated with the substructure synthesis method. Examples are presented at the end of each subsection to illustrate the concepts.

3.2.a Determination of Mass and Stiffness Matrices

The development of the structural model identification (SMI) method is introduced by starting with the simplest mathematical representation of a dynamic system, the classical undamped equations of motion

$$M \ddot{u} + K u = f \tag{3.26}$$

where M and K are the n x n mass and stiffness matrices, u is the n x 1 generalized displacement vector, and f is the n x 1 generalized force vector. The dots represent differentiation with respect to time. From Eq.(3.26) the free vibration eigenproblem is defined by

$$(K - \omega_j^2 M)\, \phi_j = 0 \tag{3.27}$$

where ω_j is the jth natural frequency and ϕ_j is the corresponding jth mode shape (eigenvector). Taking the Fourier transform of Eq.(3.26) yields the frequency response model

$$U(\omega) = [K - \omega^2 M]^{-1} F(\omega) = H(\omega)\, F(\omega) \tag{3.28}$$

where $U(\omega)$ and $F(\omega)$ are the Fourier transforms of the generalized displacement and force vectors, and $H(\omega)$ is the n x n frequency response

matrix. Note that $H(\omega)$, the frequency response matrix, should be distinguished from the block Hankel matrix H(k) of the previous section. The reader will be able to make this distinction since H(k) is discussed only in Section 3.1.b. It will be shown in the sequel that the new identification method under discussion requires the availability of any one of the following sets of measurements:

I. m ($\leq$n) natural frequencies and mode shapes and at least one element of the frequency response matrix (measured throughout the operating frequency range of the structure), or

II. m ($\leq$n) natural frequencies and one complete column (or row) of the frequency response matrix, or

III. m ($\leq$n) natural frequencies and at least one element of the frequency response matrix, with the underlying assumption that the a priori model of the structure initially provides acceptable estimates of the true mode shapes.

The first two measurement sets, although more demanding than the third, do not require the initial structural model to be "close" to the truth whereas the third set, as stated, requires the initial model to yield a reasonable approximation to the true mode shapes. A most important point to make here is that the frequency response measurements provide a unique identification of the structure, a consequence not provided by measurements of natural frequencies and mode shapes alone (due to the homogeneity of Eq.(3.27)).

The first step in the SMI method is to fit the measured frequency

response elements. From Eq.(3.28) the inverse of the frequency response matrix becomes

$$H^{-1} = [K - \omega^2 M] \tag{3.29}$$

Pre- and post-multiplying by ϕ^T and ϕ, respectively (where ϕ is defined as the n x n modal matrix normalized with respect to the (unknown) true mass matrix), yields

$$\phi^T H^{-1}(\omega)\ \phi = \phi^T [K - \omega^2 M]\ \phi \tag{3.30a}$$

$$= \Lambda - \omega^2 I \tag{3.30b}$$

In Eq.(3.30) Λ is the n x n diagonal matrix of the natural frequencies squared and I is the n x n identity matrix. Solving for $H(\omega)$ yields

$$H(\omega) = \phi\ (\Lambda - \omega^2 I)^{-1} \phi^T \tag{3.31}$$

Equation (3.31) represents the undamped special case of the spectral decomposition of the frequency response matrix [44]. A typical element of the frequency response matrix, H_{jk}, can be written from Eq.(3.31) as

$$H_{jk} = \sum_{r=1}^{n} \frac{\phi_{jr}\ \phi_{kr}}{\omega_r^2 - \omega^2} \tag{3.32}$$

First it is assumed that a subset of (m) measured natural frequencies ($\tilde{\omega}_j$), measured (or approximated) mode shapes (ψ_j), and a measured frequency response element ($\tilde{H}_{jk}(\omega)$) are available (i.e. measurement sets I or III). Since the true mass matrix is not known, the mode shapes do not represent their mass-normalized counterparts but can be related by the scaling

$$\phi_j = \sqrt{\alpha_j}\, \psi_j \qquad j=1,2,\ldots,m \tag{3.33}$$

where α_j is defined as the jth "modal normalization factor". Substituting Eq.(3.33) into Eq.(3.32), and motivated by Ewins [44], an approximation of the frequency response element can be obtained as

$$\tilde{H}_{jk} = \frac{a_1}{\omega^2} + \sum_{r=1}^{m} \left(\frac{\psi_{jr}\, \psi_{kr}}{\tilde{\omega}_r^2 - \omega^2}\, \alpha_r \right) + a_2 \tag{3.34}$$

In Eq.(3.34), the first term is introduced to represent the contribution of any unmeasured rigid-body modes ($\omega_r = 0$) and the third term is introduced to represent an approximation to the (usually small) contribution of unmeasured high-frequency modes outside the frequency range of interest ($\omega_r >> \omega$). To determine the unknown constants (a_1, a_2, α_r's), Eq.(3.34) is "sampled" at different frequencies distributed throughout the range of interest to provide the following linear system

$$\begin{Bmatrix} \tilde{H}_{jk}(\omega_1) \\ \cdot \\ \cdot \\ \cdot \\ \tilde{H}_{jk}(\omega_N) \end{Bmatrix} = \begin{bmatrix} \frac{1}{\omega_1^2} & L_{11} & L_{12} & \cdots & L_{1m} & 1 \\ \cdot & & & & & \cdot \\ \cdot & & & & & \cdot \\ \cdot & & & & & \cdot \\ \cdot & & & & & \cdot \\ \frac{1}{\omega_N^2} & L_{N1} & L_{N2} & \cdots & L_{Nm} & 1 \end{bmatrix} \begin{Bmatrix} a_1 \\ \alpha_1 \\ \alpha_2 \\ \vdots \\ \alpha_m \\ a_2 \end{Bmatrix} \tag{3.35a}$$

where $$L_{pq} = \frac{\psi_{jq}\,\psi_{kq}}{\tilde{\omega}_q^2 - \omega_p^2} \tag{3.35b}$$

Solving Eq.(3.35) for estimates of the unknown constants, by least-squares for example, determines an estimation of the mass-normalized mode shapes through Eq.(3.33).

If the measurements available contain m natural frequencies and a complete column of the frequency response matrix (i.e. measurement set II) then the frequency response elements can be approximated by the equation

$$\tilde{H}_{jk}(\omega) = \frac{a_1}{\omega^2} + \sum_{r=1}^{m} \left(\frac{r\Gamma_{jk}}{\tilde{\omega}_r^2 - \omega^2} \right) + a_2 \tag{3.36}$$

where $_r\Gamma_{jk}$ are the to-be-determined "modal constants" [44]. Similar to Eq.(3.35), the modal constants can be estimated using a least-squares solution of the following linear system

$$\begin{Bmatrix} \tilde{H}_{jk}(\omega_1) \\ \cdot \\ \cdot \\ \cdot \\ \tilde{H}_{jk}(\omega_N) \end{Bmatrix} = \begin{bmatrix} \frac{1}{\omega_1^2} & L_{11} & L_{12} & \cdots & L_{1m} & 1 \\ & \cdot & & & & \cdot \\ & \cdot & & & & \cdot \\ & \cdot & & & & \cdot \\ & \cdot & & & & \cdot \\ \frac{1}{\omega_N^2} & L_{N1} & L_{N2} & \cdots & L_{Nm} & 1 \end{bmatrix} \begin{Bmatrix} a_1 \\ {}_1\Gamma_{jk} \\ {}_2\Gamma_{jk} \\ \vdots \\ {}_m\Gamma_{jk} \\ a_2 \end{Bmatrix} \tag{3.37a}$$

where $$L_{pq} = \frac{1}{\tilde{\omega}_q^2 - \omega_p^2} \tag{3.37b}$$

To estimate the mass-normalized mode shapes requires two steps. First the point frequency response measurements, $\tilde{H}_{kk}$, are used to estimate the kth component of each mode shape,

$$\tilde{H}_{kk} \rightarrow [{}_1\Gamma_{kk}, {}_2\Gamma_{kk}, \cdots, {}_m\Gamma_{kk}] \tag{3.38a}$$

$$\rightarrow [\phi_{k1}^2, \phi_{k2}^2, \cdots, \phi_{km}^2] \tag{3.38b}$$

Then the transfer response measurements, $\tilde{H}_{jk}$, are used to estimate the remaining elements of the mode shapes,

$$\tilde{H}_{jk} \rightarrow [{}_1\Gamma_{jk}, {}_2\Gamma_{jk}, \cdots, {}_m\Gamma_{jk}] \tag{3.39a}$$

$$\rightarrow [\phi_{j1}\phi_{k1}, \phi_{j2}\phi_{k2}, \cdots, \phi_{jm}\phi_{km}] \tag{3.39b}$$

$$\rightarrow [\phi_{j1}, \phi_{j2}, \cdots, \phi_{jm}] \tag{3.39c}$$

Once the estimated normalized mode shapes have been obtained, whether from the modal normalization factors of Eq.(3.34) or from the modal constants of Eq.(3.36), the next step in the identification process is the estimation of the mass and stiffness matrices via inversion of the orthonormality conditions

$$\phi_j^T M \phi_k = \delta_{jk} \tag{3.40a}$$

$$\phi_j^T K \phi_k = \tilde{\omega}_j^2 \delta_{jk} \tag{3.40b}$$

In the unlikely case that the full n x n normalized modal matrix has been determined (m = n in Eq.(3.34) or (3.36)), the mass and stiffness matrices can be computed uniquely from

$$M = \phi^{-T} \phi^{-1} \tag{3.41a}$$

$$K = \phi^{-T} \tilde{\Lambda} \phi^{-1} \tag{3.41b}$$

In the more practical situation of having m (<n) available normalized mode shapes, submatrix scale factors are introduced to express the mass and stiffness matrices as

$$M = M_0 + \sum_{r=1}^{P} \gamma_r M_r \tag{3.42a}$$

$$K = K_0 + \sum_{r=1}^{Q} \beta_r K_r \tag{3.42b}$$

where M_0, K_0 are the initial estimates of the mass and stiffness matrices,

M_r, K_r are the rth mass and stiffness submatrices (assembled into the global coordinate system),

γ_r, β_r are the mass and stiffness submatrix scale factors, and

P, Q are the number of mass and stiffness submatrices.

Incorporating Eq.(3.42) into (3.40) and utilizing Eq.(3.33) yields

$$\psi_j^T \left[M_0 + \sum_{r=1}^{P} \gamma_r M_r\right] \psi_k = \delta_{jk} / \alpha_j \tag{3.43a}$$

$$\psi_j^T \left[K_0 + \sum_{r=1}^{Q} \beta_r K_r\right] \psi_k = \tilde{\omega}_j^2 \delta_{jk} / \alpha_j \tag{3.43b}$$

Equation (3.43) can be rearranged to provide a linear system involving the unknown submatrix scale factors as follows,

$$\begin{Bmatrix} -\psi_j^T M_0 \psi_j + \dfrac{1}{\alpha_j} \\ -\psi_j^T M_0 \psi_k \end{Bmatrix} = \begin{bmatrix} \psi_j^T M_1 \psi_j & \cdots & \psi_j^T M_P \psi_j \\ \psi_j^T M_1 \psi_k & \cdots & \psi_j^T M_P \psi_k \end{bmatrix} \begin{Bmatrix} \gamma_1 \\ \vdots \\ \gamma_P \end{Bmatrix} \tag{3.44a}$$

$$\begin{Bmatrix} -\psi_j^T K_0 \psi_j + \dfrac{\tilde{\omega}_j^2}{\alpha_j} \\ -\psi_j^T K_0 \psi_k \end{Bmatrix} = \begin{bmatrix} \psi_j^T K_1 \psi_j & \cdots & \psi_j^T K_Q \psi_j \\ \psi_j^T K_1 \psi_k & \cdots & \psi_j^T K_Q \psi_k \end{bmatrix} \begin{Bmatrix} \beta_1 \\ \vdots \\ \beta_Q \end{Bmatrix} \tag{3.44b}$$

where the second set of equations in Eqs.(3.44a) and (3.44b) are valid

when $j \neq k$. Collecting the subsets of above equations for each measured or estimated mode $(\tilde{\omega}_j, \psi_j)$ into a global set provides a linear system which can be solved to obtain a least-squares estimate of the submatrix scale factors, provided that $m(m+1)/2 \geq \max(P,Q)$. Since Eqs.(3.34) and (3.36) represent approximations to the frequency response element, an iterative procedure can be used whereby the contribution of the high-frequency unmeasured modes is a predicted function of ω (using the present best estimate of the modeled structure) and used in these equations in lieu of measurements. This means that fewer high frequency mode effects need to be approximated by the constant a_2 .

At this stage there are a few points worth noting: (i) The mass and stiffness submatrices described in Eq.(3.42) can represent a single finite element or a group of finite elements having the same assumed geometry, material properties, boundary conditions, and modeling assumptions [33]. Examination of the kinetic and potential energy contributions of each submatrix to the total energy of the initial structural model enables the analyst to neglect any submatrices which do not contribute energy to the specific modes for which measurements are available [33]. The percent contribution of each submatrix to the total kinetic and potential energy of the system can be approximated from the diagonals of the matrices $\phi_0^T M_0 \phi_0$ and $\phi_0^T K_0 \phi_0 / \omega_{0j}^2$, where ϕ_0 is the mass-normalized modal matrix of the original model. (ii) The use of scale factors in Eq.(3.42) conserves the consistency of the original finite element model in the sense that no unmodeled coupling occurs as a result of the identification process. (iii) In the event that the identified model does not reliably predict the measured responses, two

courses of action might be considered. It may be beneficial, from examination of the submatrix energy contributions, to refine (or remodel) those submatrices which provide significant energy to the measured modes of interest. This "informal" approach could prove quite practical in an actual application. A more formal approach is to examine the model parameter covariance matrix associated with the least-squares solution of Eq.(3.44) to determine which parameters (submatrix scale factors) are deemed statistically unacceptable. Model refinement can then be performed on those submatrices of interest. Although attractive in principle, practical application of this approach could prove quite difficult because the determination of the covariance matrices associated with the left side of Eq.(3.44) requires not only propagation of the covariance matrix from the estimation of the modal normalization factors, but also an estimate of the covariances associated with the modeling errors inherent in the initial model and the propagation of these errors into the approximate mode shapes.

As observed from Eq.(3.43), the measured (or approximated) modal vectors must be of dimension equal to the number of degrees of freedom of the finite element model. In practice, measurements of mode shapes cannot usually be obtained at every location on the actual structure corresponding to a degree of freedom on the structural model. To approximate the remaining elements of an incomplete modal vector, the method of *dynamic condensation* may be useful [61-62].

Consider the partitioned form of the unforced equations of motion

$$\begin{bmatrix} M_{ss} & M_{sp} \\ M_{ps} & M_{pp} \end{bmatrix} \begin{Bmatrix} \ddot{u}_s \\ \ddot{u}_p \end{Bmatrix} + \begin{bmatrix} K_{ss} & K_{sp} \\ K_{ps} & K_{pp} \end{bmatrix} \begin{Bmatrix} u_s \\ u_p \end{Bmatrix} = \begin{Bmatrix} 0 \\ 0 \end{Bmatrix} \tag{3.45}$$

which leads to the eigenproblem

$$\begin{bmatrix} K_{ss} - \omega_i^2 M_{ss} & K_{sp} - \omega_i^2 M_{sp} \\ K_{ps} - \omega_i^2 M_{ps} & K_{pp} - \omega_i^2 M_{pp} \end{bmatrix} \begin{Bmatrix} \phi_{s_i} \\ \phi_{p_i} \end{Bmatrix} = \begin{Bmatrix} 0 \\ 0 \end{Bmatrix} \tag{3.46}$$

To determine the natural frequencies and mode shapes Paz [61-62] outlines the following steps:

Step 1 An approximation of ω_i is introduced into Eq.(3.46) and $\{\phi_{s_i}\}$ is eliminated from the first partition to obtain

$$\begin{aligned} \{\phi_{s_i}\} &= -[K_{ss} - \omega_i^2 M_{ss}]^{-1}[K_{sp} - \omega_i^2 M_{sp}] \{\phi_{p_i}\} \\ &= \bar{T}_i \{\phi_{p_i}\} \end{aligned} \tag{3.47}$$

The actual modes shapes $\{\phi_i\}$ can now be approximated, given only ϕ_{p_i}, as

$$\{\phi_i\} = \begin{Bmatrix} \phi_{s_i} \\ \phi_{p_i} \end{Bmatrix} = \begin{bmatrix} \bar{T}_i \\ I \end{bmatrix} \{\phi_{p_i}\} = T_i \{\phi_{p_i}\} \tag{3.48}$$

Step 2 The reduced mass and stiffness matrices can be determined from

$$M_{iR} = T_i^T M T_i \tag{3.49a}$$

$$K_{iR} = T_i^T K T_i \tag{3.49b}$$

Step 3 The reduced eigenproblem

$$[K_{iR} - \omega^2 M_{iR}] \{\phi_p\} = \{0\} \tag{3.50}$$

can be solved to obtain an improved value of ω_i and a starting estimate of ω_{i+1}.

An iterative procedure can be employed whereby the updated value of ω_i is used in Eq.(3.47) and the process repeated. Paz shows that very accurate results can often be obtained after just one iteration.

For the identification problem, the objective is to identify the actual mass and stiffness matrices, not their reduced counterparts. If a set of incomplete measured mode shapes $\{\psi_{p_i}\}$ are available, identification can be performed as follows:

Step 1 Estimate the mode shape normalization factors using the measured frequency response elements as described in the previous subsection.

Step 2 Use the measured natural frequency, $\tilde{\omega}_i$, and the initial estimates of the mass matrix, M_0, and the stiffness matrix, K_0, to obtain the transformation matrix as given in Eqs.(3.47) and (3.48). Repeat this step for each measured natural frequency.

Step 3 Obtain the complete mode shapes from each incomplete measured mode using

$$\{\psi_i\} = T_i \{\psi_{p_i}\} \tag{3.51}$$

The mass and stiffness matrices can now be identified using Eq.(3.44).

If desired, this process can be repeated by using the updated mass and stiffness matrices in place of their initial representations in Step 2. To avoid the matrix inversions required in Eq.(3.47), a Gauss-Jordan elimination of the secondary variables in Eq.(3.46) can be performed to obtain

$$\begin{bmatrix} I & -\bar{T}_i \\ 0 & D_i \end{bmatrix} \begin{Bmatrix} \phi_{s_i} \\ \phi_{p_i} \end{Bmatrix} = \begin{Bmatrix} 0 \\ 0 \end{Bmatrix} \tag{3.52}$$

The transformation matrix can be directly obtained from Eq.(3.52) without the need for any matrix inversions [62].

The advantages of the above SMI method are:

i) incorporation of measured frequency response data provides for unique identification of the structure,

ii) the least-squares formulations for fitting the frequency response elements and for estimation of the submatrix scale factors are linear,

iii) if measurements of mode shapes or one column of the frequency response matrix are available (measurement sets I or II) the mass

and stiffness matrices of Eq.(3.42) need only be representative of the true model in the coupling of the elements (the initial numerical values of the elements can be inaccurate by an order of magnitude!),

iv) the consistency of the original finite element model is maintained (no additional off-diagonal coupling occurs as a consequence of the identification process), and

v) use of submatrix scale factors for the mass and stiffness matrix representations limits the estimation process to a relatively small set of parameters.

In the first four of the following examples, the "measurement" set consists of noise-free results obtained from analysis of the true model. Consideration of measurement noise is deferred to Example 3.5, in which various degrees of damping are also imposed on the system. To initiate the estimation process, the true model is approximated by perturbing the parameters inherent to the system.

Example 3.1 Identification of a Truss Structure

To illustrate the use of the SMI method developed in the previous section, the mass and stiffness matrices of the ten-bay planar truss structure shown in Figure 3.1 are identified. An ad hoc approximation of the true model is constructed by increasing the mass matrix elements by 10% and decreasing the stiffness matrix elements by 10%. This approximate model is used to initiate the estimation process. The "measurement" set, obtained from the solution and analysis of the true model, consists of the first eight natural frequencies, a transverse -frequency response function representing the ratio of vertical displacement at point B to vertical force at point A, and a longitudinal frequency response function representing the ratio of horizontal displacement at point B to horizontal force at point A. The current best estimate of the structural model is used to determine approximate mode shapes required for the identification process.

To cast the model in terms of mass and stiffness submatrices, the following element groups are chosen:

Group I 20 upper and lower primary bending elements

Group II 20 diagonal bending/shear elements

Group III 10 vertical column elements.

The initial fractional modal energy contributions of each element group (based upon the initial approximate model) are given in Table 3.1. It can be observed from the energy distributions that Group III contributes

only negligibly to the first eight modes and, therefore, is not used for the identification procedure. In practice, it may prove constructive to repeat these energy distribution calculations as the solution is refined.

A comparison of the "measured" natural frequencies to the initial and final estimates (after three iterations) is summarized in Table 3.2, and a comparison of the "measured" frequency response functions with their initial and final estimates is provided in Figure 3.2. It can be observed that the longitudinal frequency response function is required for detection of the fourth and the eighth modes.

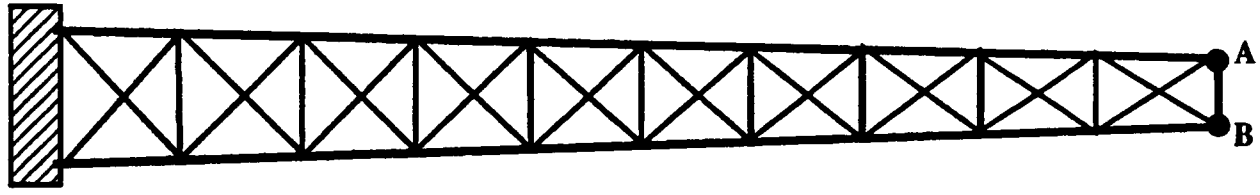

Parameters

EA_{hor} = 300,000 lb

EA_{vert} = 100,000 lb

EA_{diag} = 200,000 lb

ρ_{hor} = 0.0003 slug/in

ρ_{vert} = 0.0001 slug/in

ρ_{diag} = 0.0002 slug/in

Base Depth = 24 in

Tip Depth = 11.432 in

Length = 36 in x 10 = 360 in

Figure 3.1 Undamped Ten-Bay Truss Structure

Table 3.1 Group Energy Distributions for the Undamped Truss Structure

Mode	Kinetic Energy (%)			Potential Energy (%)		
	Group I	Group II	Group III	Group I	Group II	Group III
1	55.9	39.9	4.2	98.3	1.7	0.0
2	55.0	40.0	5.0	86.7	13.3	0.0
3	54.6	40.0	5.4	71.6	28.4	0.0
4	55.5	40.2	4.3	76.2	16.9	6.9
5	54.3	39.8	5.9	56.0	44.0	0.0
6	53.9	39.6	6.5	42.2	57.7	0.1
7	53.2	39.4	7.4	30.7	69.3	0.0
8	54.8	40.4	4.8	73.0	19.6	7.4

Table 3.2 Natural Frequency Results for the Undamped Truss Structure

MODE	$\tilde{\omega}_n$	ω_{n_o}	ω_{n_f}
1	6.76 rad/sec	6.11 rad/sec	6.79 rad/sec
2	34.77	31.45	34.88
3	87.22	78.89	87.31
4	117.93	106.67	117.82
5	157.11	142.12	156.93
6	240.50	217.54	239.74
7	333.88	302.01	332.22
8	359.58	325.25	358.87

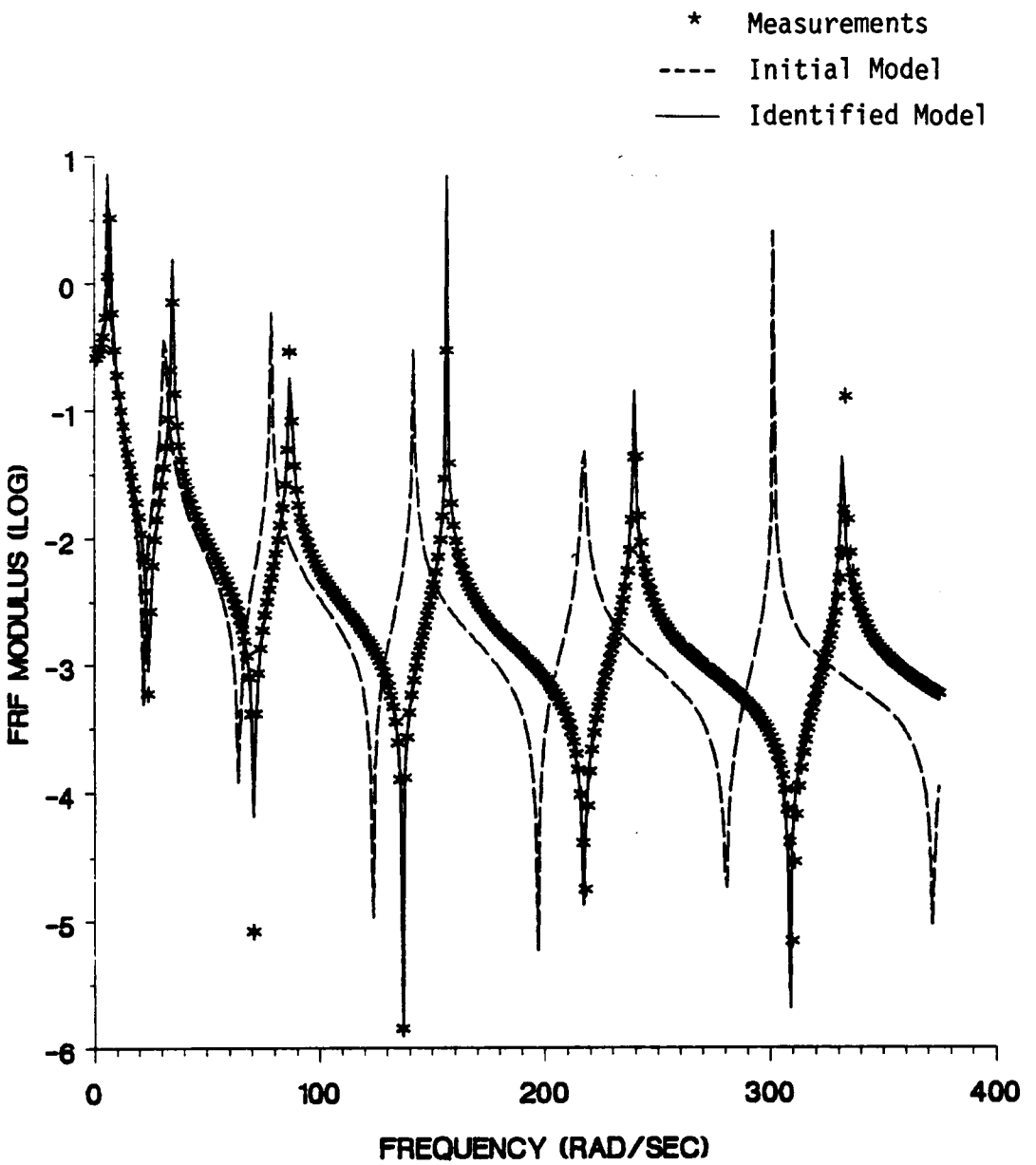

Figure 3.2a Transverse Frequency Response Results for the Undamped Truss Structure

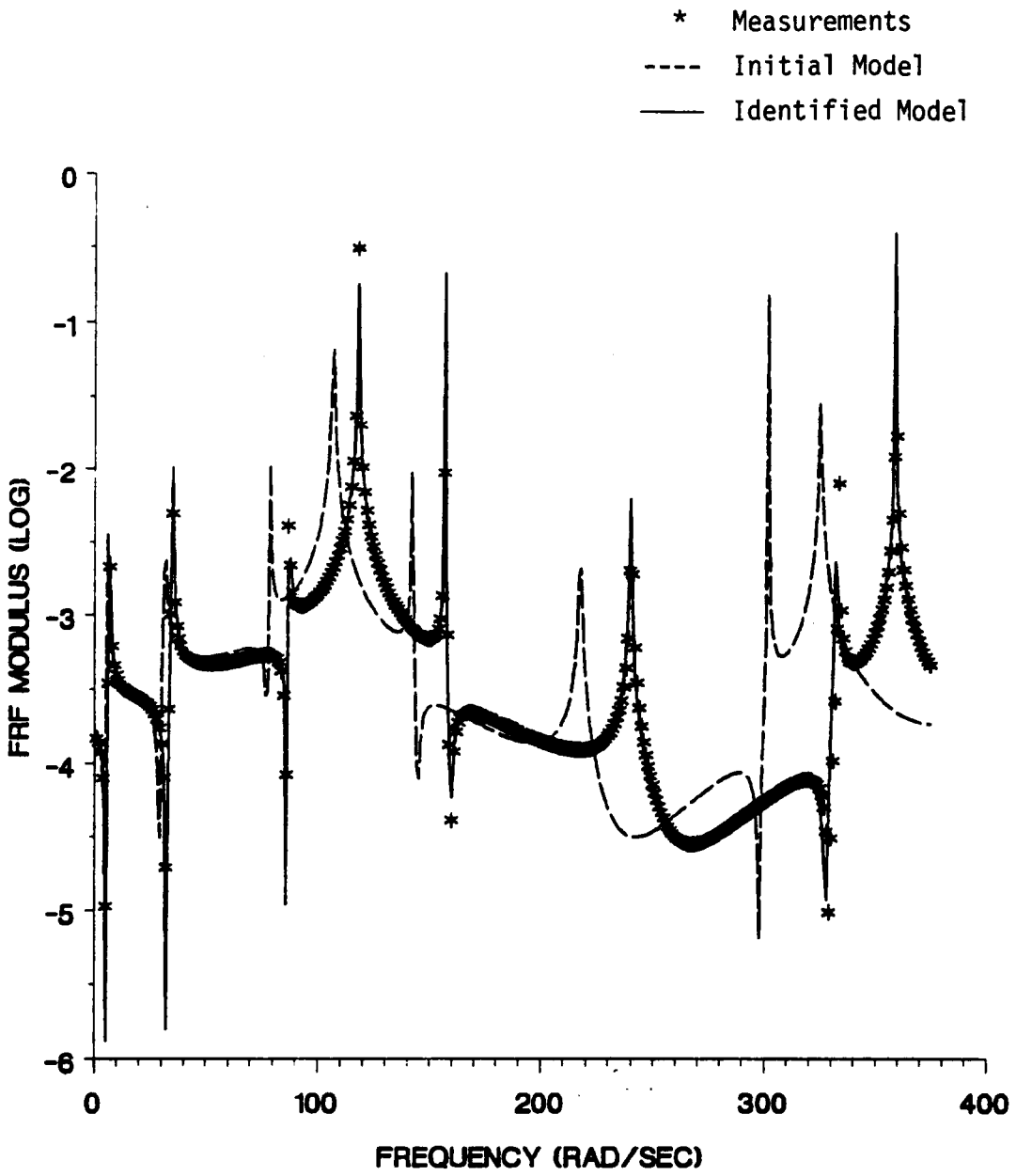

Figure 3.2b Longitudinal Frequency Response Results for the Undamped Truss Structure

Example 3.2 Identification of a Flexible Manipulator Arm

The mass and stiffness matrices are identified for the simple manipulator arm shown in Figure 3.3. The structure consists of two flexible appendages (modeled with five beam elements each), rotational springs at the base and at the connecting joint, and a grip with mass and inertia.

The true model is approximated by increasing the mass properties by 10% and decreasing the stiffness properties by 10%. The first five natural frequencies of the true model and the frequency response function representing the ratio of displacement at the joint to torque at the base are treated as measurements with approximate mode shapes determined from the current best estimate of the model.

To cast the model in terms of mass and stiffness submatrices the following element groups are chosen:

Mass ---	Group I	Mass matrix of appendage 1
	Group II	Mass matrix of appendage 2
	Group III	Tip mass moment of inertia
	Group IV	Tip mass

Stiffness ---	Group I	Stiffness matrix of appendage 1
	Group II	Stiffness matrix of appendage 2
	Group III	Base rotational stiffness
	Group IV	Joint rotational stiffness

The initial fractional modal energy contributions of each element group are given in Table 3.3. It is apparent that the first two modes approximate those that would be obtained for a two degree-of-freedom model with rigid appendages and the higher modes represent the flexibility of the appendages.

Due to the uncoupling in the energy distributions, a two step process was used to identify the structure. First, the three highest modes are used to identify mass element groups I, II, and III and stiffness element groups I and II. Then, the two lowest modes are used to identify mass element group IV and stiffness element groups III and IV. The free- and forced-response identification results (after two iterations) are provided in Table 3.4 and Figure 3.4, respectively. It is apparent that the energy distribution is an effective way to construct judicious sub-problems of reduced dimensionality. This very attractive idea, apparently first exploited by White and Maytum [33], has been found very useful in implementing the present SMI method.

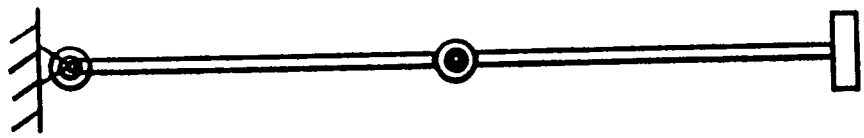

Parameters

$EI = 50{,}000$ lb·in^2	$\rho = 0.003$ slug/in
Base Spring = 10 lb·in	Joint Spring = 5 lb·in
Tip Mass = 5 slugs	Tip Inertia = 0.5 lb·in^2
Length = 25 in x 2 = 50 in	

Figure 3.3 Simple Manipulator Arm

Table 3.3 Group Energy Distributions for the Manipulator Arm

MODE	KINETIC ENERGY(%) OF MASS GROUPS				POTENTIAL ENERGY(%) OF STIFFNESS GROUPS			
	I	II	III	IV	I	II	III	IV
1	0.0	0.5	0.0	99.5	0.2	0.1	66.5	33.2
2	58.8	39.1	1.9	0.2	0.1	0.1	33.3	66.5
3	27.5	47.3	25.2	0.0	19.5	80.5	0.0	0.0
4	64.0	22.1	13.9	0.0	75.7	24.1	0.1	0.1
5	16.5	38.8	44.7	0.0	7.4	92.6	0.0	0.0

Table 3.4 Natural Frequency Results for the Manipulator Arm

MODE	$\tilde{\omega}_n$	ω_{n_o}	ω_{n_f}
1	0.0230 rad/sec	0.0209 rad/sec	0.0230 rad/sec
2	1.062	0.9617	1.066
3	55.44	50.15	55.55
4	91.12	82.42	91.19
5	156.75	141.78	156.98

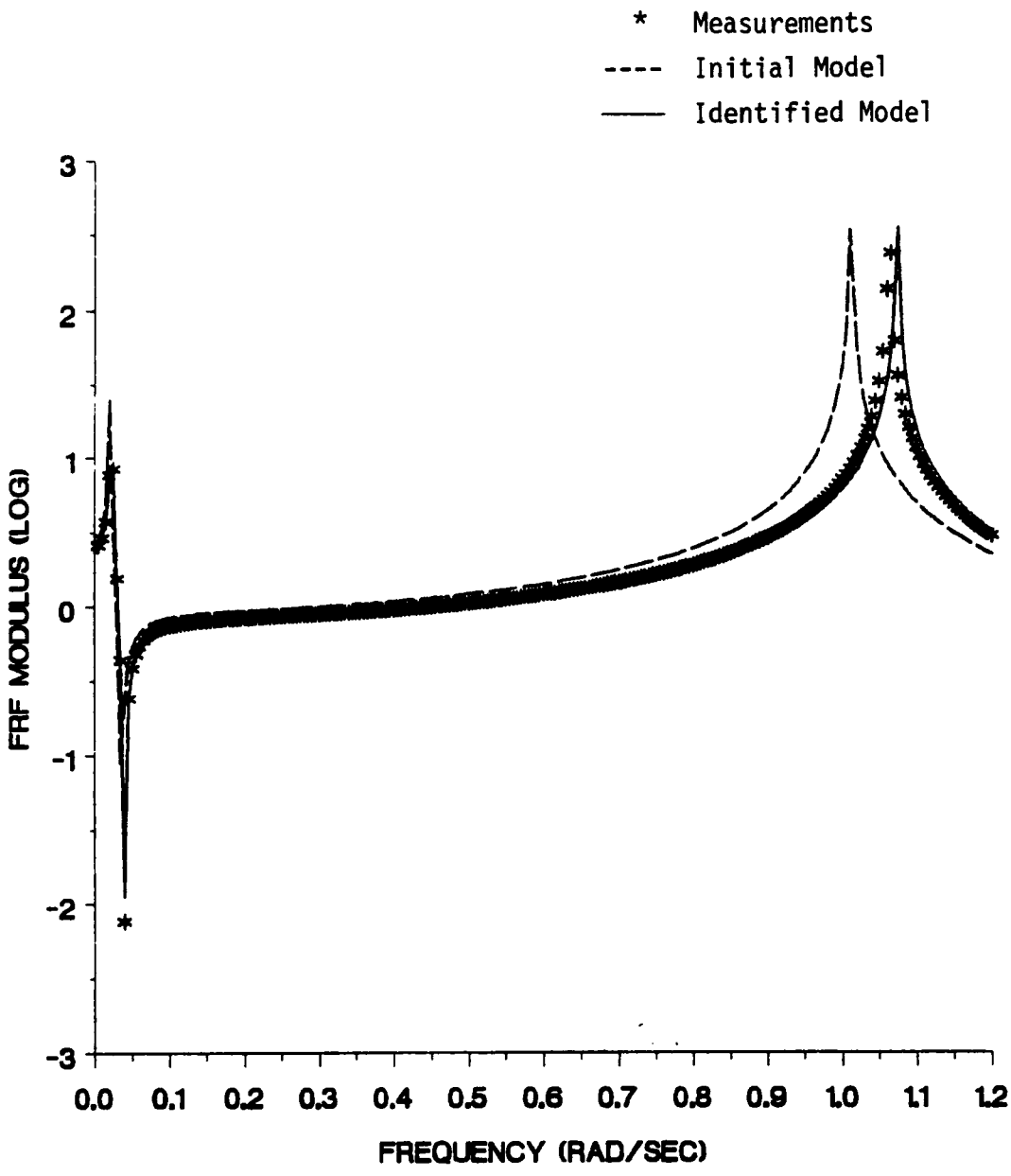

Figure 3.4a Low-Range Frequency Response Results for the Manipulator Arm

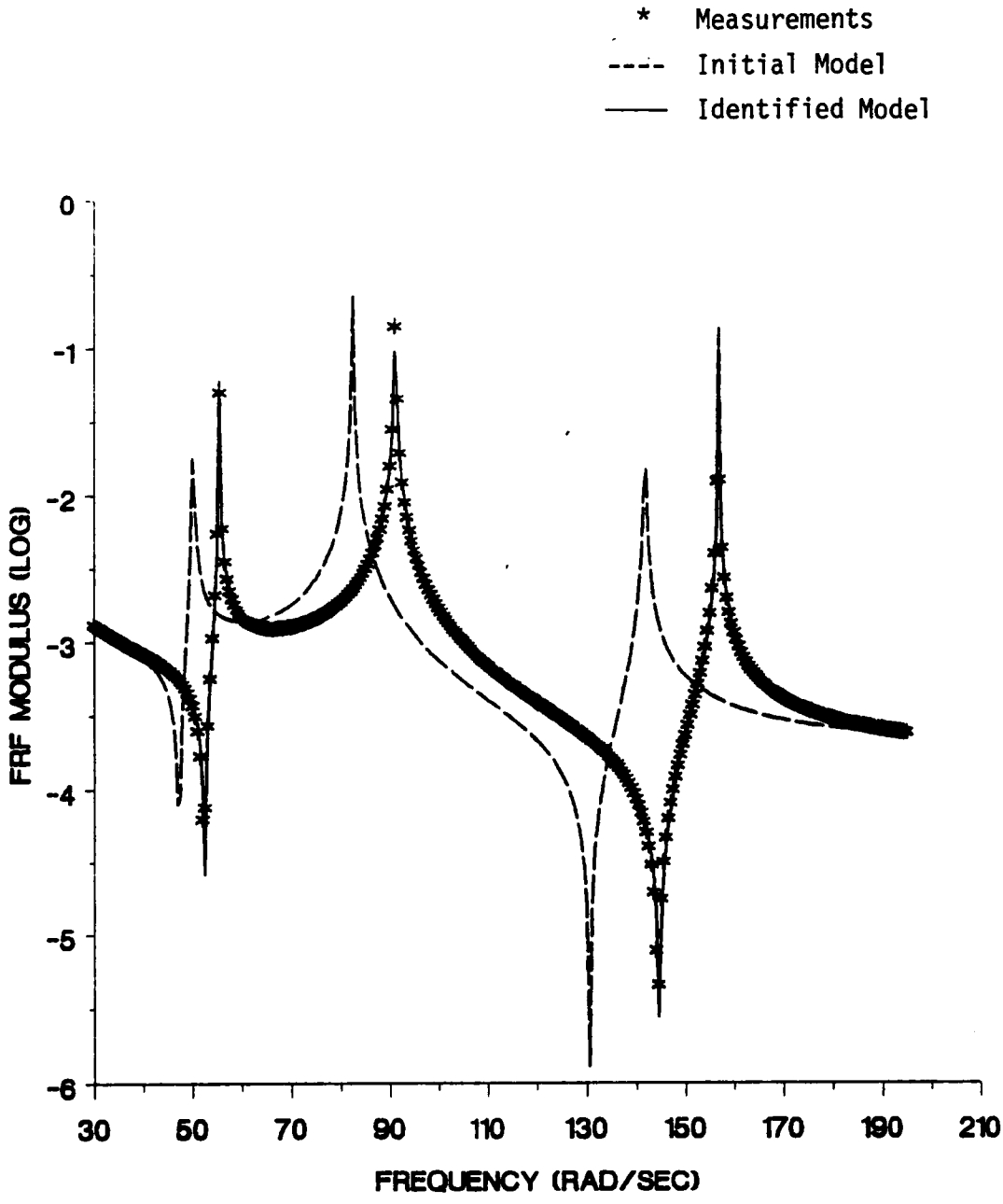

Figure 3.4b High-Range Frequency Response Results for the Manipulator Arm

3.2.b Application to Substructure Synthesis

Many large complex structures consist of a combination of several smaller components or substructures, such as the wings and fuselage of an airplane or the Space Shuttle Orbiter and its payloads. In addition, component substructures of some of these structures, including the many proposed large space structures, will likely be assembled and tested in-orbit due to the high flexibility of the assembled structure.

The *substructure synthesis* method [63-65] plays an important part in the analysis of large structures; in many cases it provides the only computationally efficient and practical approach available to the practicing engineer. It is therefore important to develop an identification scheme which is compatible with and can be efficiently integrated into the substructure synthesis method. First, the substructure synthesis method is reviewed for a very simple class of structures, then extensions to accommodate the above estimation concepts are developed.

Consider the simple beam structure given in Figure 3.5 composed of two substructures and their corresponding finite element models. The equations of motion for each substructure are given as

$$M_1\ddot{u}_1 + K_1u_1 = f_1 \tag{3.53a}$$

$$M_2\ddot{u}_2 + K_2u_2 = f_2 \tag{3.53b}$$

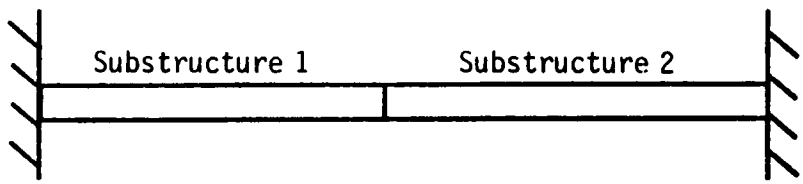

Figure 3.5 Substructures of a Simple Clamped Beam

Following Craig [64,65], two fundamental mode sets for each substructure are defined:

i) Fixed-Interface Normal Modes $\{\hat{\phi}_i^S\}$ --- free vibration mode shapes obtained from Eq.(3.53) by fixing (clamping) each interface degree of freedom.

ii) Static Constraint Modes $\{Y_i^S\}$ --- static shape functions obtained from Eqs.(3.53) by setting one interface degree of freedom to unity with all others set to zero. Each substructure in Figure 3.5 has two static constraint modes.

Applying the coordinate transformation

$$u_s = \left[\hat{\phi}^S \vdots Y^S\right] q_s = \Phi_s q_s \tag{3.54}$$

to each substructure yields the following transformed equations of motion for the system

$$M_d \ddot{q}_d + K_d q_d = f_d \tag{3.55a}$$

where

$$M_d = \begin{bmatrix} \Phi_1^T M_1 \Phi_1 & 0 \\ 0 & \Phi_2^T M_2 \Phi_2 \end{bmatrix} \tag{3.55b}$$

$$K_d = \begin{bmatrix} \Phi_1^T K_1 \Phi_1 & 0 \\ 0 & \Phi_2^T K_2 \Phi_2 \end{bmatrix} \tag{3.55c}$$

$$f_d = \begin{Bmatrix} \Phi_1^T f_1 \\ \Phi_2^T f_2 \end{Bmatrix} \tag{3.55d}$$

$$q_d = \begin{Bmatrix} q_1 \\ q_2 \end{Bmatrix} \tag{3.55e}$$

It should be noted that the fixed-interface normal modes in Φ_s are truncated at the substructure level to include only a dominant subset of modes from the finite element analysis. The next step is to impose continuity conditions on the displacement and slope at the interface. This leads to an expression of the form

$$[C_1 \quad C_2] \begin{Bmatrix} q_d^I \\ q_d^D \end{Bmatrix} = 0 \tag{3.56}$$

where q_d^I is the independent coordinate vector and q_d^D is the dependent coordinate vector (due to continuity). Solving for q_d^D yields

$$q_d^D = -C_2^{-1} C_1 q_d^I \tag{3.57}$$

so that q_d can now be written as

$$q_d = \begin{Bmatrix} q_d^I \\ q_d^D \end{Bmatrix} = \begin{bmatrix} I \\ -C_2^{-1} C_1 \end{bmatrix} q_d^I = \beta q_d^I \tag{3.58}$$

The "connected" set of equations is now defined as

$$M_c \ddot{q}_d^I + K_c q_d^I = f_c \tag{3.59a}$$

$$M_c = \beta^T M_d \beta \tag{3.59b}$$

$$K_c = \beta^T K_d \beta \tag{3.59c}$$

$$f_c = \beta^T f_d \tag{3.59d}$$

The dimension of M_c and K_c is equal to the number of retained fixed-interface normal modes plus constraint modes from each substructure minus the number of dependent coordinates due to interface continuity. The attractiveness of this method is that a reduced set of equations can be obtained for analyzing the assembled structure, leading to less computational expense without a significant loss of accuracy. The free vibration eigenproblem associated with Eq.(3.59) yields the natural frequencies, ω_i , and "connected" mode shapes, Z_i . The actual mode shapes can be approximated from the connected mode shapes using Eqs.(3.54) and (3.58),

$$\phi_i = \begin{bmatrix} \Phi_1 & 0 \\ 0 & \Phi_2 \end{bmatrix} \beta Z_i = \Phi_G \beta Z_i \tag{3.60}$$

To use the SMI method proposed in the previous section, the relation for the frequency response matrix must first be obtained. The "connected" frequency response matrix, obtained by taking the Fourier transform of Eq.(3.59), becomes

$$H_c^{-1}(\omega) = K_c - \omega^2 M_c \tag{3.61}$$

Pre- and post-multiplying by Z^T and Z, respectively, and using the orthonormality conditions

$$Z^T M_c Z = I \tag{3.62a}$$

$$Z^T K_c Z = \Lambda = \text{diag}(\omega_j^2) \tag{3.62b}$$

yields

$$H_c(\omega) = Z\,[\Lambda - \omega^2 I]^{-1} Z^T \tag{3.63}$$

The Fourier transform of Eq.(3.59) is written as

$$Q_d^I(\omega) = Z\,[\Lambda - \omega^2 I]^{-1} Z^T F_c(\omega) \tag{3.64}$$

where $Q_d^I(\omega)$ and $F_c(\omega)$ are the Fourier transforms of $q_d^I(t)$ and $f_c(t)$. Multiplying Eq.(3.64) by Φ_G and using Eqs.(3.58) and (3.59d) yields

$$Q_d(\omega) = \beta\, Z\,[\Lambda - \omega^2 I]^{-1} Z^T \beta^T F_d(\omega) \tag{3.65}$$

where $Q_d(\omega)$ and $F_d(\omega)$ are the Fourier transforms of $q_d(t)$ and $f_d(t)$. Multiplying Eq.(3.65) by Φ_G and utilizing Eqs.(3.54) and (3.55d) results in the desired relation,

$$\begin{Bmatrix} U_1(\omega) \\ U_2(\omega) \end{Bmatrix} = \Phi_G \beta\, Z\,[\Lambda - \omega^2 I]^{-1}\, Z^T \beta^T \Phi_G^T \begin{Bmatrix} F_1(\omega) \\ F_2(\omega) \end{Bmatrix} \tag{3.66a}$$

$$= \phi \, [\Lambda - \omega^2 I]^{-1} \, \phi^T \begin{Bmatrix} F_1(\omega) \\ F_2(\omega) \end{Bmatrix} \tag{3.66b}$$

$$= H(\omega) \begin{Bmatrix} F_1(\omega) \\ F_2(\omega) \end{Bmatrix} \tag{3.66c}$$

where (U_1, U_2) and (F_1, F_2) are the Fourier transforms of (u_1, u_2) and (f_1, f_2). The measured frequency response elements and the measured natural frequencies and mode shapes can now be used to determine the modal normalization factors via (see Eq.(3.34))

$$\tilde{H}_{jk}(\omega) = \frac{a_1}{\omega^2} + \sum_{r=1}^{m} \left(\frac{\psi_{jr} \, \psi_{kr}}{\tilde{\omega}_r^2 - \omega^2} \alpha_r \right) + a_2 \tag{3.67}$$

The normalization factors (α_r), obtained from a least-squares fit of Eq.(3.67), normalize the connected mode shapes with respect to the connected mass matrix, as described in Eq.(3.62). These equations can be written in terms of the measured mode shapes and the actual mass and stiffness matrices of each substructure to obtain

$$\{ {}_1\psi_j^T \;\; {}_2\psi_j^T \} \begin{bmatrix} M_1 & 0 \\ 0 & M_2 \end{bmatrix} \begin{Bmatrix} {}_1\psi_k \\ {}_2\psi_k \end{Bmatrix} = \delta_{jk} / \alpha_j \tag{3.68a}$$

$$\{ {}_1\psi_j^T \;\; {}_2\psi_j^T \} \begin{bmatrix} K_1 & 0 \\ 0 & K_2 \end{bmatrix} \begin{Bmatrix} {}_1\psi_k \\ {}_2\psi_k \end{Bmatrix} = \tilde{\omega}_j^2 \, \delta_{jk} / \alpha_j \tag{3.68b}$$

where ${}_1\psi_j$ is that portion of the jth measured mode shape containing the coordinates of substructure 1, and ${}_2\psi_j$ is that portion of the jth

measured mode shape containing the coordinates of substructure 2. The mass and stiffness matrices of each substructure can now be identified in the following manner. First the substructure mass and stiffness matrices are expanded, using submatrix scale factors, to obtain

$$M_1 = {}_1M_0 + \sum_{r=1}^{P1} {}_1\gamma_r \, {}_1M_r \tag{3.69a}$$

$$M_2 = {}_2M_0 + \sum_{r=1}^{P2} {}_2\gamma_r \, {}_2M_r \tag{3.69b}$$

$$K_1 = {}_1K_0 + \sum_{r=1}^{Q1} {}_1\beta_r \, {}_1K_r \tag{3.69c}$$

$$K_2 = {}_2K_0 + \sum_{r=1}^{Q2} {}_2\beta_r \, {}_2K_r \tag{3.69d}$$

Equation (3.69) is then used in Eq.(3.68) to obtain a set of equations for determining the mass submatrix scale factors,

$$\begin{Bmatrix} -{}_1\psi_j^T \, {}_1M_0 \, {}_1\psi_j - {}_2\psi_j^T \, {}_2M_0 \, {}_2\psi_j + \dfrac{1}{\alpha_j} \\ \\ -{}_1\psi_j^T \, {}_1M_0 \, {}_1\psi_k - {}_2\psi_j^T \, {}_2M_0 \, {}_2\psi_k \end{Bmatrix} = \begin{bmatrix} {}_1J_j & {}_2J_j \\ \\ {}_1J_{jk} & {}_2J_{jk} \end{bmatrix} \begin{Bmatrix} {}_1\gamma_1 \\ \vdots \\ {}_1\gamma_{P1} \\ {}_2\gamma_1 \\ \vdots \\ {}_2\gamma_{P2} \end{Bmatrix} \tag{3.70a}$$

where $${}_iJ_j = \text{row}\{{}_i\psi_j^T \, {}_iM_1 \, {}_i\psi_j \;,\; {}_i\psi_j^T \, {}_iM_2 \, {}_i\psi_j \;,\ldots.\} \qquad i=1,2 \tag{3.70b}$$

$${}_iJ_{jk} = \text{row}\{{}_i\psi_j^T \, {}_iM_1 \, {}_i\psi_k \;,\; {}_i\psi_j^T \, {}_iM_2 \, {}_i\psi_k \;,\ldots.\} \qquad i=1,2 \tag{3.70c}$$

and the stiffness submatrix scale factors,

$$\begin{Bmatrix} -{}_1\psi_j^T\ {}_1K_0\ {}_1\psi_j - {}_2\psi_j^T\ {}_2K_0\ {}_2\psi_j + \dfrac{\tilde{\omega}_j^2}{\alpha_j} \\ \\ -{}_1\psi_j^T\ {}_1K_0\ {}_1\psi_k - {}_2\psi_j^T\ {}_2K_0\ {}_2\psi_k \end{Bmatrix} = \begin{bmatrix} {}_1J_j & {}_2J_j \\ \\ {}_1J_{jk} & {}_2J_{jk} \end{bmatrix} \begin{Bmatrix} {}_1\beta_1 \\ \vdots \\ {}_1\beta_{Q1} \\ {}_2\beta_1 \\ \vdots \\ {}_2\beta_{Q2} \end{Bmatrix} \tag{3.71a}$$

where $${}_iJ_j = \text{row}\{{}_i\psi_j^T\ {}_iK_1\ {}_i\psi_j\ ,\ {}_i\psi_j^T\ {}_iK_2\ {}_i\psi_j\ ,\ldots\} \qquad i=1,2 \tag{3.71b}$$

$${}_iJ_{jk} = \text{row}\{{}_i\psi_j^T\ {}_iK_1\ {}_i\psi_k\ ,\ {}_i\psi_j^T\ {}_iK_2\ {}_i\psi_k\ ,\ldots\} \qquad i=1,2 \tag{3.71c}$$

The second set of equations in Eqs.(3.70) and (3.71) is valid when $j \neq k$. Collecting the set of above equations for each measured mode results in a linear least-squares formulation for determining the submatrix scale factors of each substructure provided, as a necessary condition, that $m(m+1)/2$ is greater than $\max(P1+P2, Q1+Q2)$. In summary, it has been shown that the structural model identification method developed in Section 3.2.a can easily be applied to a substructure synthesis model. Using modal measurements and frequency response measurements from the final assembled structure, the modal normalization factors are first estimated, and the mass and stiffness matrices of each substructure are then identified simultaneously, using a "stacked" version of the orthonormality conditions, as presented in Eq.(3.68).

Example 3.3 Identification of a Clamped Beam

The mass and stiffness matrices of the clamped beam given in Figure. 3.6 are identified using the component mode synthesis method described in the previous section. The true model for the structure is approximated by increasing the mass densities by 10% and decreasing the bending rigidities by 10%. The first four natural frequencies of the true model and the point frequency response function at location A are treated as measurements with approximate mode shapes determined from the current best estimate of the model.

The component mode synthesis model consists of three substructures containing five beam elements in each. To determine the final connected model two modes are kept from the fixed-interface eigensolutions of each separate substructure. The mass and stiffness matrices of each substructure are chosen as submatrices so that there exist a total of three mass scale factors and three stiffness scale factors to be identified.

A comparison of the "measured" natural frequencies with the initial and final estimates (after two iterations) is provided in Table 3.5. A comparison of the "measured" and estimated frequency response function is provided in Figure 3.7.

It should be noted that identification of a standard fifteen-element model of the beam required three times more computational expense than identification of the component mode model. For large structures, the order reduction and computational savings implicit in this approach may prove vital in making identification practical.

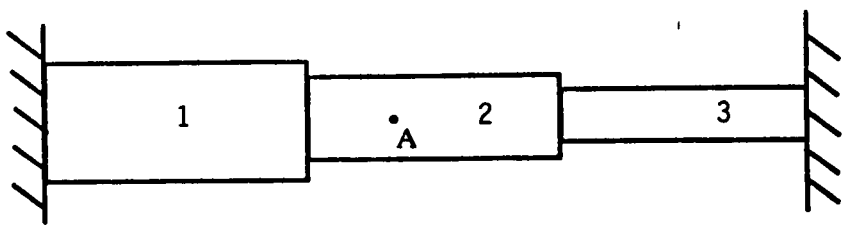

Parameters

EI_1= 833,333 lb·in^2 ρ_1= 0.003 slug/in

EI_2= 263,672 lb·in^2 ρ_2= 0.002 slug/in

EI_3= 52,083 lb·in^2 ρ_3= 0.001 slug/in

Length = 50 in x 3 = 150 in

Figure 3.6 Clamped Beam Structure

Table 3.5 Natural Frequency Results for the Component Mode Clamped Beam

MODE	$\tilde{\omega}_n$	ω_{n_o}	ω_{n_f}
1	10.94 rad/sec	12.10 rad/sec	10.93 rad/sec
2	28.96	32.01	28.85
3	60.58	66.98	60.42
4	94.84	105.01	94.85

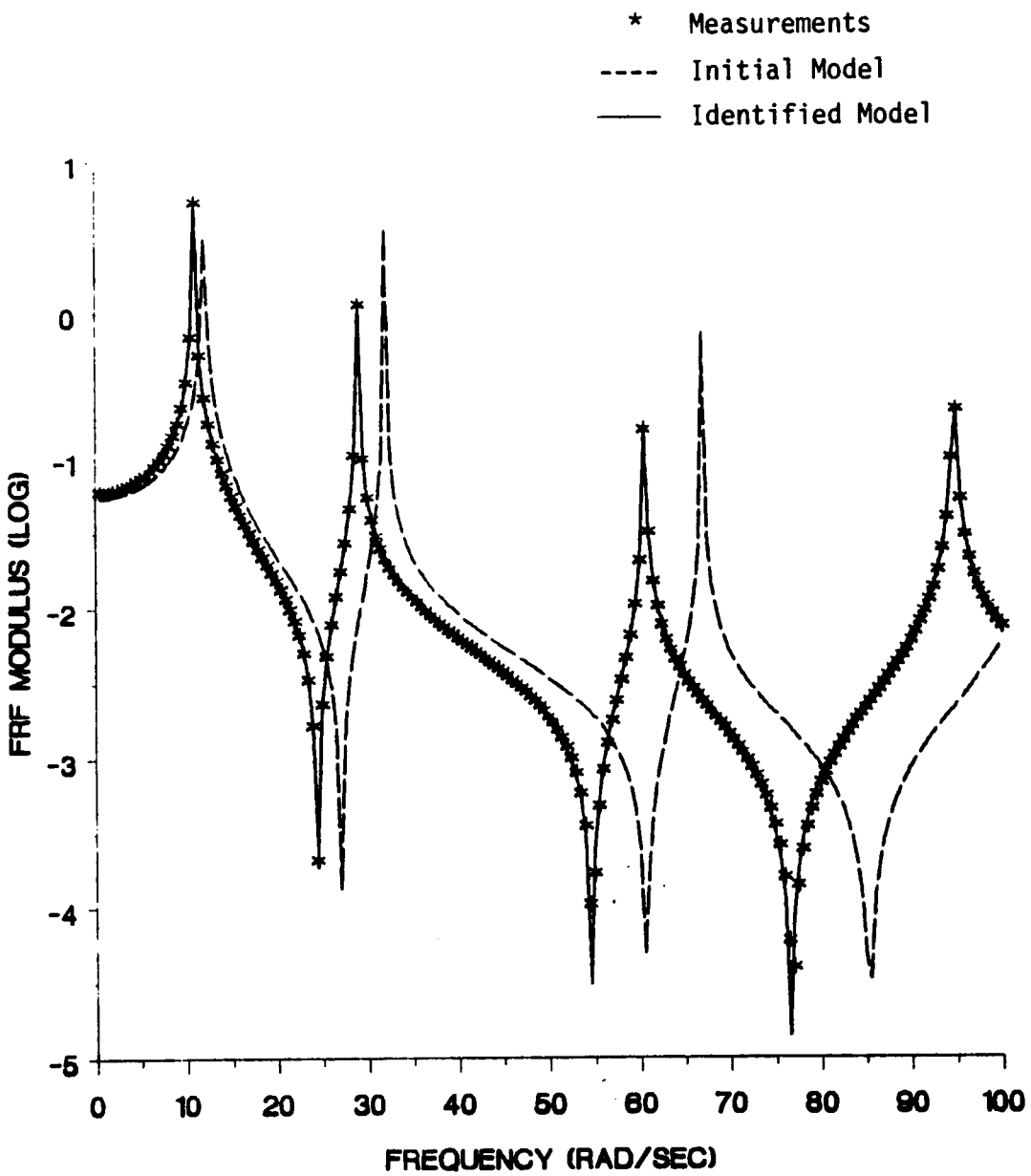

Figure 3.7 Frequency Response Results for the Clamped Beam

3.3 Structural Model Identification of Viscous Damped Structures

In the previous section a structural identification method is presented for and applied to undamped (or negligibly damped) structures. In this section the SMI method is extended to include viscous-damped structures. While all structures exhibit a certain amount of passive damping due to internal molecular friction, energy loss in connecting joints, and/or atmospheric resistance, the combined effects often result in a system with "light" damping. For many applications an undamped analysis may be adequate, but certainly not in the vicinity of resonant conditions. Also, systems under active control (i.e. state feedback control) can exhibit as much artificial damping as the controller is designed to produce. Figure 3.8 shows a comparison of the frequency response function of a system with no damping, with light damping, and with heavy damping. It can be observed that the frequency response function for the lightly damped structure differs significantly from the undamped structure only near resonant conditions, whereas the response of the heavily damped structure differs from the undamped structure throughout a significant portion of the frequency range. In the first subsection, the SMI method is extended to apply to generally-damped structures in state space; a matrix perturbation method for identification of lightly-damped structures in configuration space is developed in the second subsection.

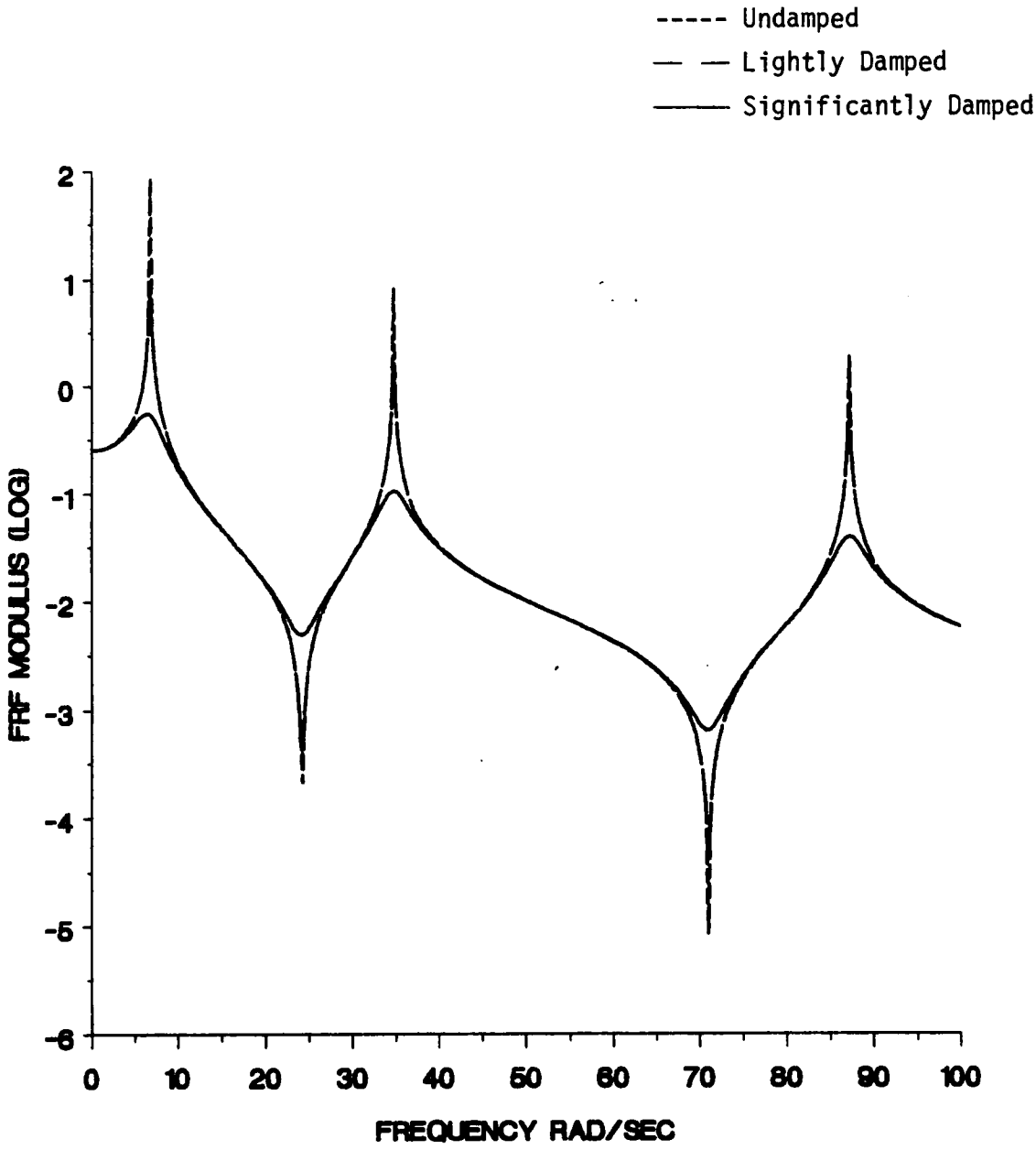

Figure 3.8 Typical Frequency Response Functions for Various Degrees of Damping

3.3.a A State Space Approach for General Linear Damping

When significant damping is present in a structure, due to passive and/or active sources, the configuration-space identification method developed in Section 3.2 must be revised. The three measurement sets discussed in Section 3.2.a remain the same for a general viscous-damped structure except that the natural frequencies and mode shapes are now the more general complex-valued eigenvalues and eigenvectors, leading to the complex-valued frequency response matrix.

The equations of motion in configuration-space take on the well-known form

$$M\ddot{u} + C\dot{u} + Ku = f \tag{3.72}$$

where C is the n x n viscous damping matrix. If state feedback control is used to actively control the structure the force vector can be written as

$$f = f_e + f_c = f_e + Dv \tag{3.73}$$

where f_e is the n x 1 external force vector, f_c is the n x 1 control force vector, D is the n x ℓ control influence matrix and v is the ℓ x 1 input vector. The input vector (e.g. generalized forces) can be written (for a special case of linear feedback control), using the ℓ x ℓ symmetric positive definite gain matrices G_1 and G_2, in the following manner [66,67]

$$v = - G_1 D^T \dot{u} - G_2 D^T u \tag{3.74}$$

so that the closed-loop controlled system becomes

$$M\ddot{u} + C\dot{u} + Ku = f_e \tag{3.75a}$$

$$C = C_p + DG_1D^T = C_p + C_A \tag{3.75b}$$

$$K = K_p + DG_2D^T = K_p + K_A \tag{3.75c}$$

where C_p and K_p are the passive (structural) damping and stiffness matrices and C_A and K_A are the active damping and stiffness matrices due to the feedback control law of Eq.(3.74). Since M, C, and K are positive definite matrices, it can easily be shown that the class of feedback controls of Eq.(3.74) is stabilizing. The n second-order equations can be written in the 2n symmetrical state space form

$$A \begin{Bmatrix} \dot{u} \\ \ddot{u} \end{Bmatrix} + B \begin{Bmatrix} u \\ \dot{u} \end{Bmatrix} = \begin{Bmatrix} 0 \\ f_e \end{Bmatrix} \tag{3.76a}$$

where $$A = \begin{bmatrix} -K & 0 \\ 0 & M \end{bmatrix} \tag{3.76b}$$

$$B = \begin{bmatrix} 0 & K \\ K & C \end{bmatrix} \tag{3.76c}$$

The advantage of the symmetrical state space form is that the system

left and right eigenvectors are identical; this gives rise to certain simplifications and makes the first order form of the eigenvalue problem more analogous to the undamped second order form. The 2n eigenvalues and eigenvectors of the corresponding free vibration equations take on the form

$$\lambda_j = \sigma_j + i\omega_j \quad , \quad \lambda_j^* = \sigma_j - i\omega_j \qquad j=1,2,\ldots,n \tag{3.77}$$

$$\hat{\phi}_j = \begin{Bmatrix} \phi_j \\ \lambda_j \phi_j \end{Bmatrix} \quad , \quad \hat{\phi}_j^* = \begin{Bmatrix} \phi_j^* \\ \lambda_j^* \phi_j^* \end{Bmatrix} \qquad j=1,2,\ldots,n \tag{3.78}$$

where σ_j (≥ 0) is the jth damping term, ω_j is the jth damped natural frequency, ϕ_j is the jth displacement mode shape, and * represents the complex conjugate operation. The 2n x 2n modal matrix is now defined as

$$\Phi = \left[\hat{\phi}_1 \; \hat{\phi}_2 \cdots \hat{\phi}_n \vdots \hat{\phi}_1^* \; \hat{\phi}_2^* \cdots \hat{\phi}_n^*\right] \tag{3.79}$$

The frequency response matrix for this system is obtained from the Fourier transform of Eq.(3.76),

$$\begin{Bmatrix} U(i\omega) \\ i\omega\, U(i\omega) \end{Bmatrix} = [i\omega A + B]^{-1} \begin{Bmatrix} 0 \\ F_e(i\omega) \end{Bmatrix} \tag{3.80a}$$

$$= H(i\omega) \begin{Bmatrix} 0 \\ F_e(i\omega) \end{Bmatrix} \tag{3.80b}$$

where $H(i\omega)$ is the 2n x 2n complex-valued frequency response matrix. Using the orthonormality conditions

$$\phi^T A \phi = I \tag{3.81a}$$

$$\phi^T B \phi = -\Lambda = -\text{diag}(\lambda_j) \tag{3.81b}$$

and proceeding analogous to Section 3.2.a, the state space spectral decomposition of the frequency response matrix becomes

$$H(i\omega) = \phi\,[i\omega I - \Lambda]^{-1}\phi^T \tag{3.82}$$

A typical element of the matrix can be written from Eq.(3.82) as

$$H_{jk}(i\omega) = \sum_{r=1}^{n} \left(\frac{\phi_{jr}\,\phi_{kr}}{i\omega - \lambda_r} + \frac{\phi_{jr}^{*}\,\phi_{kr}^{*}}{i\omega - \lambda_r^{*}} \right) \tag{3.83}$$

It is first assumed that a set of m ($\leq$n) measured eigenvalues ($\tilde{\lambda}_j$) and measured (or approximated) eigenvectors (ψ_j) , and a measured frequency response element ($\tilde{H}_{jk}$) are available. Using Eq.(3.33) in Eq.(3.83) yields an approximation of the frequency response element,

$$\tilde{H}_{jk} = \frac{a_1}{i\omega} + \sum_{r=1}^{m} \left(\frac{\psi_{jr}\,\psi_{kr}}{i\omega - \tilde{\lambda}_r}\,\alpha_r + \frac{\psi_{jr}^{*}\,\psi_{kr}^{*}}{i\omega - \tilde{\lambda}_r^{*}}\,\alpha_r^{*} \right) + a_2 \tag{3.84}$$

As in Eq.(3.34), the first term represents any rigid-body modes present in the system and the last term represents an approximation to the unmeasured high-frequency modes. Equation (3.84) can now be "sampled" at various frequency levels to obtain a linear least-squares estimation of the unknown parameters. To improve the estimation process the definition $\alpha_r = \alpha_r^R + i\alpha_r^I$ is used so that the sampled equations take on the form

$$\begin{Bmatrix} \tilde{H}_{jk}(i\omega_1) \\ \vdots \\ \tilde{H}_{jk}(i\omega_N) \end{Bmatrix} = \begin{bmatrix} \frac{1}{i\omega_1} & L_{11} \cdots L_{1m} & \hat{L}_{11} \cdots \hat{L}_{1m} & 1 \\ \vdots & \ddots & \ddots & \vdots \\ \frac{1}{i\omega_N} & L_{N1} \cdots L_{Nm} & \hat{L}_{N1} \cdots \hat{L}_{Nm} & 1 \end{bmatrix} \begin{Bmatrix} a_1 \\ {}^{R}\alpha_1 \\ \vdots \\ {}^{I}\alpha_m \\ a_2 \end{Bmatrix} \quad (3.85a)$$

where

$$L_{pq} = \frac{\psi_{jq}\,\psi_{kq}}{i\omega_p - \lambda_q} + \frac{\psi^*_{jq}\,\psi^*_{kq}}{i\omega_p - \lambda^*_q} \quad (3.85b)$$

$$\hat{L}_{pq} = i\left[\frac{\psi_{jq}\,\psi_{kq}}{i\omega_p - \lambda_q} - \frac{\psi^*_{jq}\,\psi^*_{kq}}{i\omega_p - \lambda^*_q} \right] \quad (3.85c)$$

Equation (3.85) can now be solved for the unknown constants. If the measurements available contain m eigenvalues and a complete column of the frequency response function then the frequency response elements can be approximated using the relationship

$$\tilde{H}_{jk}(i\omega) = \frac{a_1}{i\omega} + \sum_{r=1}^{m} \left(\frac{{}^{r}\Gamma_{jk}}{i\omega - \tilde{\lambda}_r} + \frac{{}^{r}\Gamma^*_{jk}}{i\omega - \tilde{\lambda}^*_r} \right) + a_2 \quad (3.86)$$

where ${}^{r}\Gamma_{jk}$ are the complex-valued modal constants [44]. To estimate the unknown modal constants the definition ${}^{r}\Gamma_{jk} = {}^{r}\Gamma^{R}_{jk} + i\,{}^{r}\Gamma^{I}_{jk}$ is used so that the sampled equations take on the form

$$\begin{Bmatrix} \tilde{H}_{jk}(i\omega_1) \\ \vdots \\ \tilde{H}_{jk}(i\omega_N) \end{Bmatrix} = \begin{bmatrix} \frac{1}{i\omega_1} & L_{11} \cdots L_{1m} & \hat{L}_{11} \cdots \hat{L}_{1m} & 1 \\ \vdots & \ddots & \ddots & \vdots \\ \frac{1}{i\omega_N} & L_{N1} \cdots L_{Nm} & \hat{L}_{N1} \cdots \hat{L}_{Nm} & 1 \end{bmatrix} \begin{Bmatrix} a_1 \\ {}^{R}\Gamma_{jk} \\ \vdots \\ {}^{I}\Gamma_{jk} \\ a_2 \end{Bmatrix} \quad (3.87a)$$

where

$$L_{pq} = \frac{1}{i\omega_p - \tilde{\lambda}_q} + \frac{1}{i\omega_p - \tilde{\lambda}_q^*} \tag{3.87b}$$

$$\hat{L}_{pq} = i\left[\frac{1}{i\omega_p - \tilde{\lambda}_q} - \frac{1}{i\omega_p - \tilde{\lambda}_q^*}\right] \tag{3.87c}$$

The correctly normalized eigenvectors can now be obtained using Eqs.(3.38) and (3.39).

The next step is to use the orthonormality conditions of Eq.(3.81) to identify the mass, damping, and stiffness matrices. Similar to Eq.(3.42), the damping matrix is expanded as

$$C = C_0 + \sum_{r=1}^{R} \xi_r C_r \tag{3.88}$$

where C_0 is the initial estimate of the damping matrix, C_r is the rth damping submatrix, ξ_r is the rth damping submatrix scale factor, and R is the number of damping submatrices. It should be noted here that if state feedback control of the form given in Eq.(3.74) is used, some of the submatrix scale factors for both the damping and stiffness matrices can represent elements of the gain matrices in Eq.(3.74). This suggests an interesting possibility to simultaneously estimate effective linear control gains along with the structural identification.

Incorporating Eqs.(3.42), (3.88), and (3.33) into Eq.(3.81) yields

$$[\psi_j^T \quad \lambda_j\psi_j^T] \begin{bmatrix} -K_0 - \sum_{r=1}^{Q} \beta_r K_r & 0 \\ 0 & M_0 + \sum_{r=1}^{P} \gamma_r M_r \end{bmatrix} \begin{Bmatrix} \psi_k \\ \lambda_k\psi_k \end{Bmatrix} = \delta_{jk}/\alpha_j \qquad (3.89a)$$

$$[\psi_j^T \quad \lambda_j\psi_j^T] \begin{bmatrix} 0 & K_0 + \sum_{r=1}^{Q} \beta_r K_r \\ K_0 + \sum_{r=1}^{Q} \beta_r K_r & C_0 + \sum_{r=1}^{R} \xi_r C_r \end{bmatrix} \begin{Bmatrix} \psi_k \\ \lambda_k\psi_k \end{Bmatrix} = -\tilde{\lambda}_j\delta_{jk}/\alpha_j \qquad (3.89b)$$

Equations (3.89a) and (3.89b) can be combined and rearranged to form the resulting equations

$$\begin{Bmatrix} \psi_j^T(K_0 - \lambda_j^2 M_0)\ \psi_j + \dfrac{1}{\alpha_j} \\ -\psi_j^T(\lambda_j^2 C_0 + 2\lambda_j K_0)\ \psi_j - \dfrac{\tilde{\lambda}_j}{\alpha_j} \end{Bmatrix} = \begin{bmatrix} J_{1j} & J_{2j} & J_{3j} \end{bmatrix} \begin{Bmatrix} \gamma_1 \\ \vdots \\ \beta_1 \\ \vdots \\ \xi_1 \\ \vdots \end{Bmatrix} \qquad (3.90a)$$

$$\begin{Bmatrix} \psi_j^T(K_0 - \lambda_j\lambda_k M_0)\ \psi_k \\ -\psi_j^T[\lambda_j\lambda_k C_0 + (\lambda_j + \lambda_k)\ K_0]\ \psi_k \end{Bmatrix} = \begin{bmatrix} J_{1jk} & J_{2jk} & J_{3jk} \end{bmatrix} \begin{Bmatrix} \gamma_1 \\ \vdots \\ \beta_1 \\ \vdots \\ \xi_1 \\ \vdots \end{Bmatrix} \qquad (3.90b)$$

where

$$J_{1j} = \begin{bmatrix} \lambda_j^2\ \psi_j^T M_1 \psi_j & \lambda_j^2\ \psi_j^T M_2 \psi_j & \cdots \\ 0 & 0 & \cdots \end{bmatrix} \qquad (3.90c)$$

$$J_{2j} = \begin{bmatrix} -\psi_j^T K_1 \psi_j & -\psi_j^T K_2 \psi_j & \cdots \\ 2\lambda_j \psi_j^T K_1 \psi_j & 2\lambda_j \psi_j^T K_2 \psi_j & \cdots \end{bmatrix} \qquad (3.90d)$$

$$J_{3j} = \begin{bmatrix} 0 & 0 & \cdots \\ \lambda_j^2 \psi_j^T C_1 \psi_j & \lambda_j^2 \psi_j^T C_2 \psi_j & \cdots \end{bmatrix} \tag{3.90e}$$

$$J_{1jk} = \begin{bmatrix} \lambda_j \lambda_k \psi_j^T M_1 \psi_k & \lambda_j \lambda_k \psi_j^T M_2 \psi_k & \cdots \\ 0 & 0 & \cdots \end{bmatrix} \tag{3.90f}$$

$$J_{2jk} = \begin{bmatrix} -\psi_j^T K_1 \psi_k & -\psi_j^T K_2 \psi_k & \cdots \\ (\lambda_j + \lambda_k)\, \psi_j^T K_1 \psi_k & (\lambda_j + \lambda_k)\, \psi_j^T K_2 \psi_k & \cdots \end{bmatrix} \tag{3.90g}$$

$$J_{3jk} = \begin{bmatrix} 0 & 0 & \cdots \\ \lambda_j \lambda_k \psi_j^T C_1 \psi_k & \lambda_j \lambda_k \psi_j^T C_2 \psi_k & \cdots \end{bmatrix} \tag{3.90h}$$

The last two sets of equations are valid when $j \neq k$. Collecting the set of above equations for each measured eigenvalue permits a linear least-squares solution provided that $2m(2m+1) > P+Q+R$. As described in Section 3.2.a, an iterative procedure can be utilized with the current best estimates of the unmeasured high-frequency modes used as simulated replacements for their measurements.

Example 3.4 Identification of an Actively-Controlled Rotating Blade

The mass, damping, and stiffness matrices of the rotating helicopter blade shown in Figure 3.9 are identified using the state space SMI method. The damping matrix is a consequence of velocity-proportional feedback control at the blade tip (see Eq.(3.75b)).

The "measurement" set consists of the first three complex eigenvalues and the complex frequency response function at point A. To cast the model in terms of submatrices, the following element groups are chosen:

Group I	Global mass matrix
Group II	Stiffness contribution from the flexibility of the blade
Group III	Stiffness contribution from the rotation of the blade
Group IV	Actuator gain element at the blade tip

The true model is initially approximated by decreasing the mass matrix by 10%, increasing the stiffness matrix by 10%, and decreasing the actuator gain element by 5%. The free- and forced-response identification results are presented in Table 3.6 and Figure 3.10, respectively.

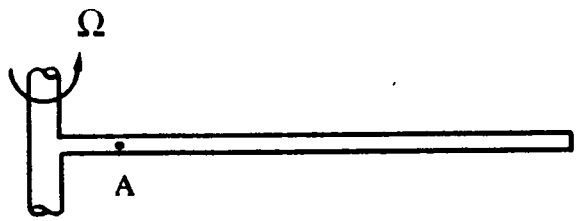

Parameters

EI = 30,000 lb·in^2 ρ = 0.0009 slug/in

Length = 100 in Ω = 5 rad/sec

Actuator Gain = 0.005

Figure 3.9 Rotating Helicopter Blade

Table 3.6 Eigenvalue Results for the Actively-Controlled Rotating Blade

MODE	MEASURED EIGENVALUE	INITIAL ESTIMATED EIGENVALUE	FINAL ESTIMATED EIGENVALUE
1	-1.019 + 5.687i	-1.088 + 5.769i	-1.015 + 5.689i
2	-1.285 + 17.842i	-1.333 + 18.808i	-1.280 + 17.849i
3	-1.155 + 41.365i	-1.212 + 44.661i	-1.151 + 41.377i

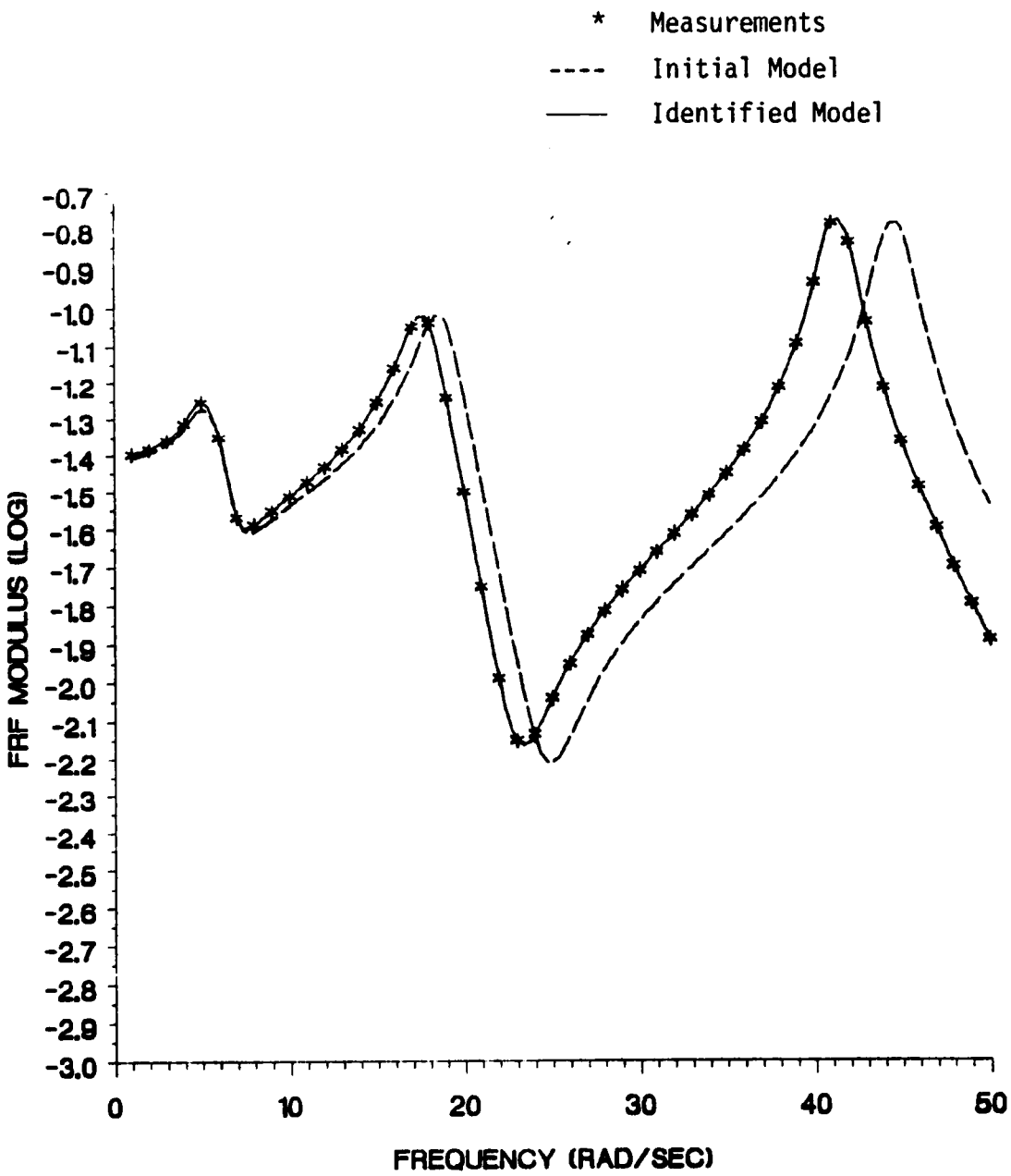

Figure 3.10 Frequency Response Results for the Rotating Blade

3.3.b A Perturbation Approach for Light Damping

When there is only a small amount of damping present in a structure the SMI method developed in Section 3.2 can be used, in conjunction with matrix perturbation theory, to identify the mass, damping, and stiffness matrices. As shown in this section, the attractive advantage of the perturbation approach is that identification can be performed in configuration space rather than state space.

Consider the undamped equations of motion in configuration space

$$M\ddot{u} + K u = f \tag{3.91}$$

for which the free-response solution yields the real system natural frequencies ω_r and mode shapes ϕ_r. Now consider the symmetrical state-space representation of Eq.(3.91) in the form

$$A \begin{Bmatrix} \dot{u} \\ \ddot{u} \end{Bmatrix} + B \begin{Bmatrix} u \\ \dot{u} \end{Bmatrix} = \begin{Bmatrix} 0 \\ f \end{Bmatrix} \tag{3.92a}$$

where

$$A = \begin{bmatrix} -K & 0 \\ 0 & M \end{bmatrix} \tag{3.92b}$$

$$B = \begin{bmatrix} 0 & K \\ K & 0 \end{bmatrix} \tag{3.92c}$$

The free-response solution to Eq.(3.92) yields the complex system eigenvalues and eigenvectors

$$\lambda_r = i\omega_r \quad , \quad \lambda_r^* = -i\omega_r \tag{3.93}$$

$$\hat{\phi}_r = \begin{Bmatrix} \phi_r \\ i\omega_r\phi_r \end{Bmatrix} \quad , \quad \hat{\phi}_r^* = \begin{Bmatrix} \phi_r \\ -i\omega_r\phi_r \end{Bmatrix} \tag{3.94}$$

If light viscous damping is introduced into the equations of motion in the form of the damping matrix C, the state-space representation is perturbed by the relation

$$B = \begin{bmatrix} 0 & K \\ K & 0 \end{bmatrix} + \begin{bmatrix} 0 & 0 \\ 0 & C \end{bmatrix} = B_0 + B_1 \tag{3.95}$$

where B_1 becomes the perturbation matrix due to the presence of the light damping. A first-order perturbation solution to the free-response eigenvalue problem of Eq.(3.92) can be obtained to approximate the change in the eigenvalues due to the inclusion of the damping matrix [68].

Consider the eigenvalue problem

$$-\lambda_{0r} A_0 \hat{\phi}_{0r} = B_0 \hat{\phi}_{0r} \tag{3.96}$$

where A_0 and B_0 are 2n x 2n symmetric matrices and λ_{0r} and $\hat{\phi}_{0r}$ are the 2n eigenvalues and eigenvectors, respectively. It is assumed that the eigenvectors are normalized such that

$$\hat{\phi}_{0j}^T A_0 \hat{\phi}_{0k} = \delta_{jk} \tag{3.97a}$$

$$\hat{\phi}_{0j}^T B_0 \hat{\phi}_{0k} = -\lambda_{0k}\delta_{jk} \tag{3.97b}$$

If small perturbations A_1 and B_1 are added to each matrix the resulting eigenvalue problem becomes

$$-\lambda_r A \hat{\Phi}_r = B \hat{\Phi}_r \tag{3.98a}$$

where
$$A = A_0 + A_1 \tag{3.98b}$$
$$B = B_0 + B_1 \tag{3.98c}$$
$$\lambda_r = \lambda_{0r} + \lambda_{1r} \tag{3.98d}$$
$$\hat{\Phi}_r = \hat{\Phi}_{0r} + \hat{\Phi}_{1r} \tag{3.98e}$$

The eigenvalues λ_{1r} and eigenvectors $\hat{\Phi}_{1r}$ represent small perturbations from their original values. Expanding Eq.(3.98a), utilizing Eq.(3.96), and neglecting second-order terms, yields the equation

$$B_1\hat{\Phi}_{0r} + B_0\hat{\Phi}_{1r} = -\lambda_{0r}A_1\hat{\Phi}_{0r} - \lambda_{0r}A_0\hat{\Phi}_{1r} - \lambda_{1r}A_0\hat{\Phi}_{0r} \tag{3.99}$$

Multiplying Eq.(3.99) by $\hat{\Phi}_{0s}^T$ and utilizing Eq.(3.97) yields the relation

$$\hat{\Phi}_{0s}^T B_1\hat{\Phi}_{0r} + \hat{\Phi}_{0s}^T B_0\hat{\Phi}_{1r} = -\lambda_{0r}\hat{\Phi}_{0s}^T A_1\hat{\Phi}_{0r} - \lambda_{0r}\hat{\Phi}_{0s}^T A_0\hat{\Phi}_{1r} - \lambda_{1r}\delta_{rs} \tag{3.100}$$

It can be observed from Eq.(3.98) that if A_1 and B_1 are zero then $\lambda_{1r} = 0$ $(r=1,2,\ldots,2n)$ and $\hat{\Phi}_{1r}$ becomes a scalar multiple of $\hat{\Phi}_{0r}$. In general, $\hat{\Phi}_{1r}$ can be written as a linear combination of the vectors $\hat{\Phi}_{01}, \hat{\Phi}_{02}, \ldots, \hat{\Phi}_{02n}$. To guarantee that $\hat{\Phi}_{1r} = 0$ when A_1 and B_1

are zero it is assumed that the perturbation eigenvector has the form [68]

$$\hat{\Phi}_{1s} = \sum_{k=1}^{2n} \varepsilon_{sk} \hat{\Phi}_{0k} \qquad \varepsilon_{ss} = 0 \qquad s=1,2,\ldots,2n \tag{3.101}$$

Using Eq.(3.101) in Eq.(3.100) and letting s=r results in an expression for the perturbed eigenvalues,

$$\lambda_{1r} = -\hat{\Phi}_{0r}^{T}[\lambda_{0r}A_1 + B_1]\,\hat{\Phi}_{0r} \qquad r=1,2,\ldots,2n \tag{3.102}$$

In the sequel, it is shown that Eq.(3.102) can be used as the central equation for identification of the damping matrix.

Referring to Figure 3.8, it is observed that the frequency response function of a lightly-damped structure closely resembles that of the undamped structure except near the resonant conditions. Therefore, given a set of complex frequency response measurements from a lightly-damped structure, identification of the mass and stiffness matrices can be performed, as described in Section 3.2, by using the real components of the frequency response measurements and the imaginary components of the eigenvalue measurements. Again, this method is only accurate for frequency response measurements away from the resonant conditions. Once the mass and stiffness matrices have been identified, the damping matrix can be determined as follows. First, the perturbed eigenvalues λ_{1r} are obtained by simply subtracting the modeled eigenvalues λ_{0r} from the measured eigenvalues $\tilde{\lambda}_r$,

$$\lambda_{1r} = \tilde{\lambda}_r - \lambda_{0r} = (\tilde{\sigma}_r + i\tilde{\omega}_r) - (i\omega_{0r}) \tag{3.103a}$$

$$= \tilde{\sigma}_r + i(\tilde{\omega}_r - \omega_{0r}) \tag{3.103b}$$

where the notation from Eq.(3.77) is used. To utilize Eq.(3.102) the eigenvectors $\hat{\phi}_{0r}$ must be normalized according to Eq.(3.97). In general, the form of the eigenvectors becomes

$$\hat{\phi}_{0r} = \begin{Bmatrix} \phi_{0r} \\ i\omega_{0r}\phi_{0r} \end{Bmatrix} \tag{3.104}$$

where ϕ_{0r} are the mode shapes from the identified undamped model, normalized with respect to the identified mass matrix. Therefore, using Eq.(3.104) in (3.97) determines scale factors α_r necessary to normalize ϕ_{0r} such that Eq.(3.97) is satisfied,

$$\alpha_r \{\phi_{0r}^T \quad i\omega\phi_{0r}^T\} \begin{bmatrix} -K & 0 \\ 0 & M \end{bmatrix} \begin{Bmatrix} \phi_{0r} \\ i\omega_{0r}\phi_{0r} \end{Bmatrix} = 1 \tag{3.105a}$$

or $$\alpha_r(-\phi_{0r}^T K \phi_{0r} - \omega_{0r}^2 \phi_{0r}^T M \phi_{0r}) = 1 \tag{3.105b}$$

or $$\alpha_r = -\frac{1}{2\omega_{0r}^2} \tag{3.105c}$$

The normalized eigenvectors Φ_{0r} can now be written as

$$\Phi_{0r} = \frac{i}{\sqrt{2}\,\omega_{0r}} \begin{Bmatrix} \phi_{0r} \\ i\omega_{0r}\phi_{0r} \end{Bmatrix} \tag{3.106}$$

Expanding the damping matrix according to Eq.(3.88), and using Eqs.(3.106) and (3.103b) in Eq.(3.102) with $A_1 = 0$ and B_1 defined in Eq.(3.95), yields the relation

$$\tilde{\sigma}_r + i(\tilde{\omega}_r - \omega_{0r}) = -\tfrac{1}{2}\, \phi_{0r}^T [C_0 + \sum_{q=1}^{Q} \xi_q C_q]\, \phi_{0r} \tag{3.107}$$

where ϕ_{0r} is the rth mass-normalized mode shape and C_q is the qth damping submatrix. Since the right side of Eq.(3.107) is real, the first-order perturbation solution does not predict a change in the undamped natural frequencies due to the addition of the light damping and, therefore, only the measured damping factors $\tilde{\sigma}_r$ are used to identify the damping matrix. Rearranging Eq.(3.107) to solve for the submatrix scale factors ξ_q yields the least-squares problem

$$\begin{Bmatrix} -2\tilde{\sigma}_1 - \phi_{01}^T C_0 \phi_{01} \\ \vdots \\ -2\tilde{\sigma}_m - \phi_{0m}^T C_0 \phi_{0m} \end{Bmatrix} = \begin{bmatrix} \phi_{01}^T C_1 \phi_{01} & \cdots & \phi_{01}^T C_Q \phi_{01} \\ \vdots & \ddots & \vdots \\ \phi_{0m}^T C_1 \phi_{0m} & \cdots & \phi_{0m} C_Q \phi_{0m} \end{bmatrix} \begin{Bmatrix} \xi_1 \\ \vdots \\ \xi_Q \end{Bmatrix} \tag{3.108}$$

where it is assumed that there are m (>Q) measured damping factors. Solving Eq.(3.108) for the submatrix scale factors leads to the desired damping matrix via Eq.(3.88). The advantages of this perturbation approach are twofold: identification of the damped equations of motion can be performed in configuration space without the need to solve the state-space eigenvalue problem, and the original damping matrix C_0 need

only represent the true damping matrix in the coupling of the elements (as a consequence of linearity, the original numerical values can be off by orders of magnitude).

Example 3.5 Identification of a Damped Truss Structure

The mass, damping, and stiffness matrices of the truss structure shown in Figure 3.11 are identified using the methods developed in the previous sections. Both internal (material) and external (atmospheric) light viscous damping is present, although there is no a priori quantification of the amount of damping. Also, actuators located at position A are available for providing velocity-proportional feedback control.

The "measurement" set consists of the first eight complex eigenvalues and the complex frequency response functions between points A and B for the uncontrolled (open-loop) system (similar to Example 3.1) and the first eight complex eigenvalues of the controlled (closed-loop) system. In this example, all complex eigenvalue and frequency response measurements are corrupted with random Gaussian noise to simulate measurement errors. To cast the model in terms of submatrices, the following element groups are chosen:

Mass and Stiffness ---	Group I	20 upper and lower bending elements
	Group II	20 diagonal bending/shear elements
Damping --- Group I		External viscous damping matrix
Group II		Internal viscous damping matrix
Group III		Transverse actuator gain element at point A

Group IV Longitudinal actuator gain element at point A

The true mass and stiffness matrices are approximated by increasing the mass by 10% and decreasing the stiffness by 10%. The actuator gain elements are also initially perturbed from their true values (see Table 3.9). The initial approximations of the external and internal passive damping matrices are only accurate in the coupling of the elements (the numerical values are off by orders of magnitude).

The identification process is carried out in three steps: (i) identification of the mass and stiffness matrices from the real components of the measured frequency response functions and the imaginary components of the measured eigenvalues of the open-loop system, using the method described in Section 3.2.a, (ii) identification of Groups I and II of the damping matrix from the real components of the measured eigenvalues of the open-loop system, using the perturbation method of Section 3.3.b, and (iii) identification of the gain elements of the damping matrix from the measured eigenvalues of the closed-loop controlled system, using the method described in Section 3.3.a.

The free- and forced-response identification results for the open-loop system are presented in Table 3.7 and Figure 3.12, respectively. The free-response identification results for the controlled system and the identified actuator gain elements are presented in Tables 3.8 and 3.9, respectively. Due to the presence of the measurement noise, the true model is not fully recovered; however, the initial estimate of the model is considerably improved.

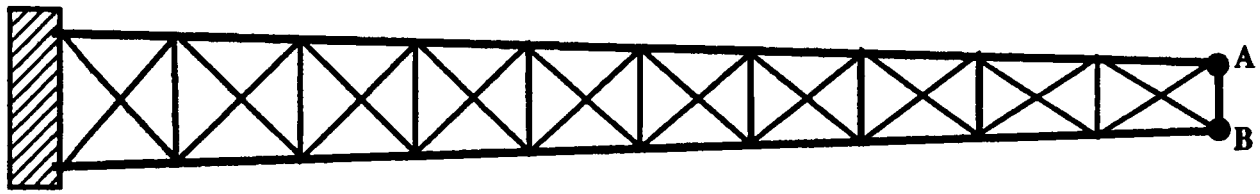

Parameters

EA_{hor} = 300,000 lb

EA_{vert} = 100,000 lb

EA_{diag} = 200,000 lb

Base Depth = 24 in

ρ_{hor} = 0.0003 slug/in

ρ_{vert} = 0.0001 slug/in

ρ_{diag} = 0.0002 slug/in

Tip Depth = 11.432 in

Length = 36 in x 10 = 360 in

Internal Damping Coefficient = 0.0001 lb·sec/in^2

External Damping Coefficient = 0.0004 lb·sec/in

Longitudinal Actuator Gain = 0.150

Transverse Actuator Gain = 0.300

Figure 3.11 Damped Ten-Bay Truss Structure

Table 3.7 Eigenvalue Results for the Lightly Damped Truss Structure

MODE	$\tilde{\lambda}$	λ_0	λ_f
1	-0.0872 + 6.73i	6.11i	-0.0872 + 6.93i
2	-0.0890 + 34.59i	31.45i	-0.0888 + 35.46i
3	-0.0891 + 87.58i	78.89i	-0.0898 + 88.29i
4	-0.1042 + 117.11i	106.67i	-0.1039 + 119.39i
5	-0.0907 + 156.49i	142.12i	-0.0906 + 157.86i
6	-0.0914 + 240.33i	217.54i	-0.0915 + 240.05i
7	-0.0929 + 332.09i	302.00i	-0.0925 + 331.39i
8	-0.1039 + 359.29i	325.25i	-0.1042 + 363.28i

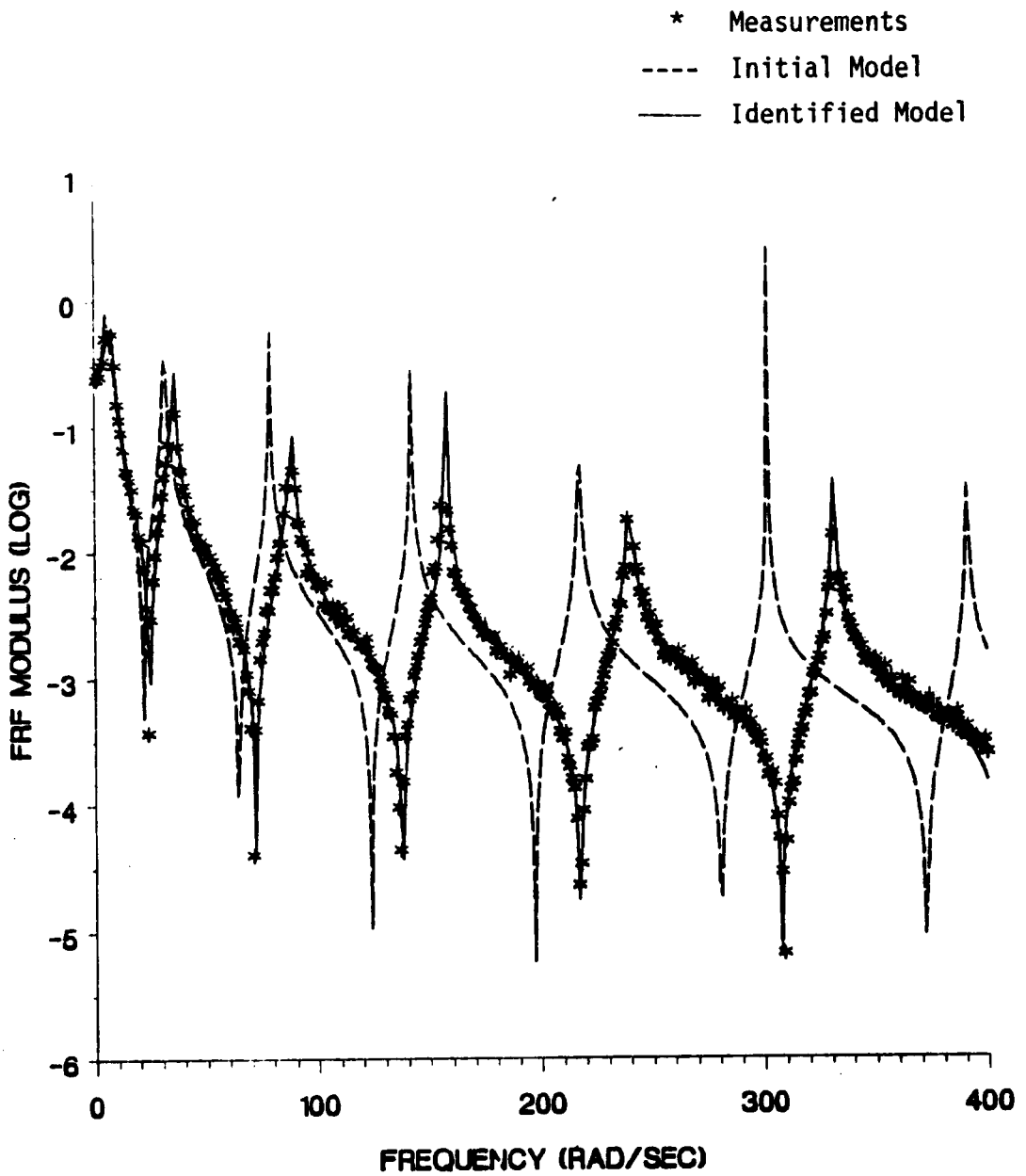

3.12a Transverse Frequency Response Results for the Lightly Damped Truss Structure

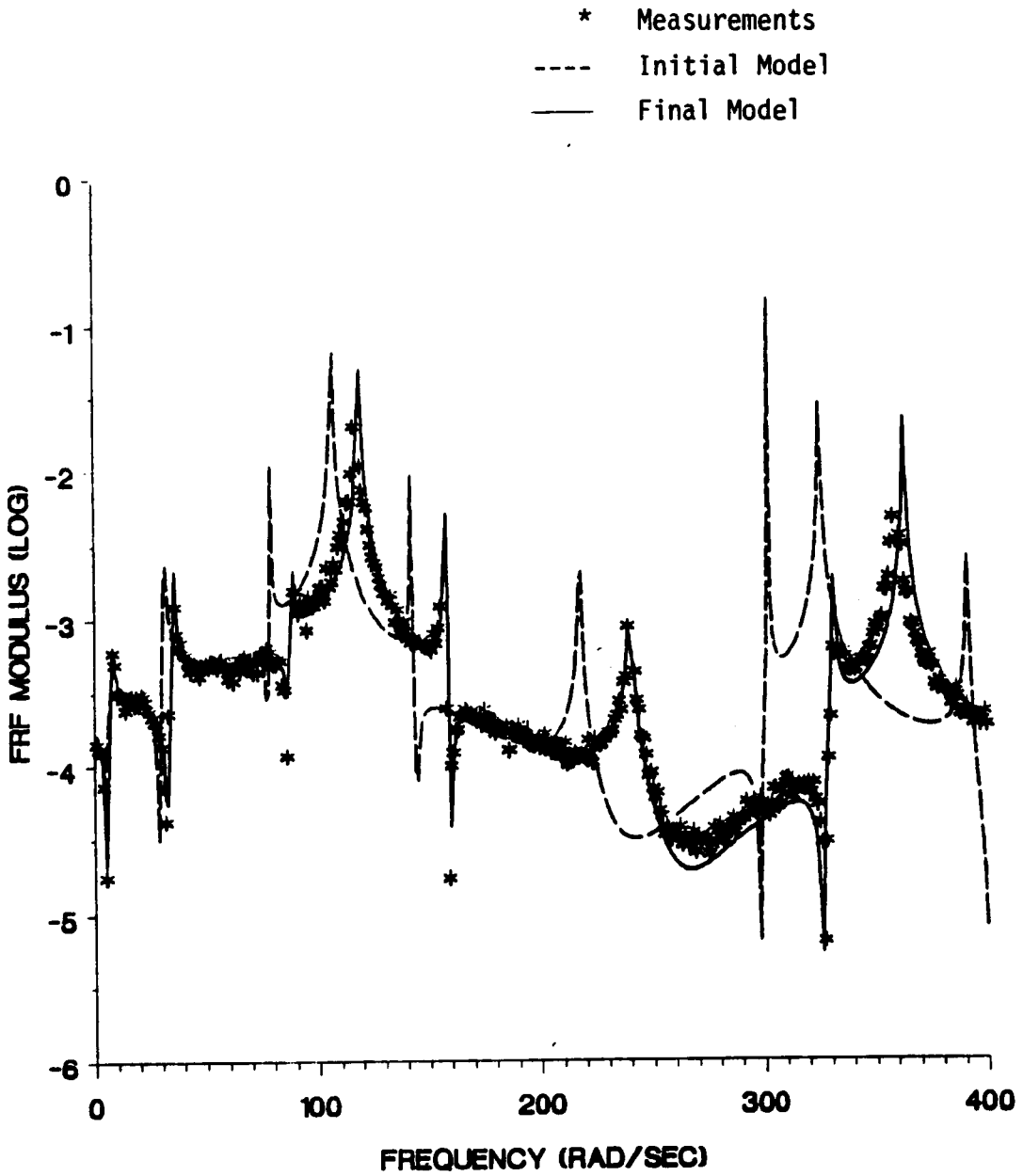

Figure 3.12b Longitudinal Frequency Response Results for the Lightly Damped Truss Structure

Table 3.8 Eigenvalue Results for the Actively-Controlled Truss Structure

MODE	$\tilde{\lambda}$	λ_0	λ_f
1	-1.766 + 6.62i	-2.098 + 6.53i	-1.601 + 6.64i
2	-1.793 + 34.06i	-2.110 + 34.68i	-1.625 + 34.78i
3	-1.735 + 86.14i	-2.053 + 87.25i	-1.585 + 87.32i
4	-0.482 + 117.16i	-0.403 + 117.94i	0.498 + 117.94i
5	-1.700 + 155.39i	-1.989 + 157.00i	-1.541 + 157.05i
6	-1.678 + 235.26i	-1.964 + 239.93i	-1.527 + 239.98i
7	-1.668 + 331.56i	-1.938 + 332.54i	-1.512 + 332.58i
8	-0.481 + 359.88i	-0.404 + 359.23i	-0.499 + 359.23i

Table 3.9 Identified Actuator Gain Elements for the Actively-Controlled Truss Structure

GAIN	TRUE VALUE	INITIAL VALUE	IDENTIFIED VALUE
$g_{A_{Long}}$	0.150	0.120	0.158
$g_{A_{Tran}}$	0.300	0.360	0.273

4. IDENTIFICATION OF LINEAR VISCOELASTIC STRUCTURES

In the previous chapter a structural model identification method is developed for undamped and viscous damped linear elastic structures. Many structural components, ranging from large aircraft wings and helicopter blades to small connecting truss joints, are being manufactured from fiber-reinforced composite materials, high-temperature thermoplastics, and other polymeric materials which exhibit potentially non-negligible (although slowly varying) viscoelastic properties or degrading elastic properties. In the first section of this chapter, a brief review of some common modeling and dynamic analysis techniques for viscoelastic structures is presented. A simple, yet practical, parameter estimation method which assumes time-localized linear elastic behavior is presented in the second section.

4.1 Dynamic Analysis of Viscoelastic Structures

The classical approach to modeling viscoelastic materials is to systematically combine spring and dashpot elements to form "chain-like" constitutive models [69,72]. The classical Kelvin and Maxwell chains for an arbitrary viscoelastic material are shown in Figure 4.1. The general constitutive equation (referred to as the "standard model") for either a Kelvin or Maxwell material is given by

$$p_0\sigma + p_1\dot{\sigma} + p_2\ddot{\sigma} + \ldots = q_0\varepsilon + q_1\dot{\varepsilon} + q_2\ddot{\varepsilon} + \ldots \qquad (4.1a)$$

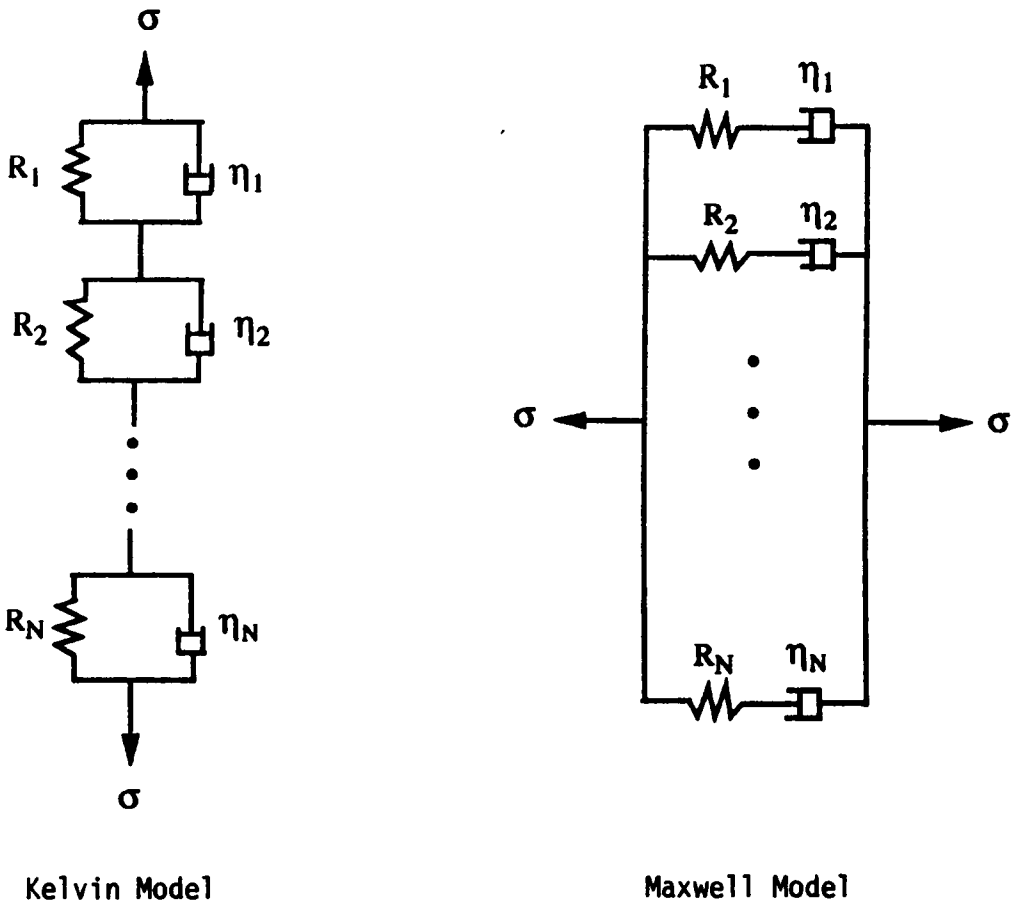

Kelvin Model

Maxwell Model

Figure 4.1 Kelvin and Maxwell Chains

or $$\sum_{r=0}^{m} p_r \frac{d^r \sigma}{dt^r} = \sum_{r=0}^{n} q_r \frac{d^r \varepsilon}{dt^r} \tag{4.1b}$$

or $$P\{\sigma\} = Q\{\varepsilon\} \tag{4.1c}$$

where σ represents the stress field, ε represents the strain field, and $P\{\ \}$ and $Q\{\ \}$ are differential operators. Halylohner [70] utilizes Eq.(4.1) in a finite element formulation to determine the transient analysis of viscoelastic bodies. The equations of motion are formulated and solved in the Laplace domain and numerically inverted to the time domain. Knowledge of the order of the operators $P\{\ \}$ and $Q\{\ \}$ and the values of the parameters is required. Hendricks [71] analyzes the motion of a three-parameter viscoelastic rotating shaft. A perturbation solution to the equations of motion is used to separate the response into short-term elastic motion and long-term viscoelastic motion. The equilibrium path of the shaft is plotted over a long period of time for various rotating frequencies.

The relaxation modulus, E(t), for the general Maxwell chain can be represented as a sum of decay exponentials [72]

$$E(t) = E_\infty + \sum_{r=1}^{N} E_r e^{-p_r t} \tag{4.2}$$

where E_∞ is the long-term modulus, E_r is the rth decay modulus, and p_r (≥ 0) is the rth relaxation time constant. Yamada, et. al. [73] utilize Eq.(4.2) to determine the response of a viscoelastic system to harmonic excitation. The equations of motion are formulated and solved in the frequency domain to determine the complex frequency response

function. The values of the parameters in Eq.(4.2) must be determined experimentally or estimated.

Another method of modeling viscoelastic materials is through use of the hereditary integral [69,72], defined for a uniaxial stress state as

$$\sigma(t) = \int_0^t E(t-\tau) \frac{d\varepsilon(\tau)}{d\tau} d\tau \tag{4.3}$$

Pinnamaneni and Makadam [74] utilize Eq.(4.3) to determine the response of a viscoelastic rocket motor. The relaxation modulus is chosen to have the form given in Eq.(4.2). Integro-differential, time-domain equations of motion are numerically solved to obtain the response.

If the relaxation modulus is written as $E(t) = E_\infty + G(t)$, the hereditary integral becomes

$$\sigma(t) = E_\infty \varepsilon(t) + \int_0^t G(t-\tau) \frac{d\varepsilon(\tau)}{d\tau} d\tau \tag{4.4}$$

Buhariwala [75] uses the three-dimensional counterpart of Eq.(4.4) to obtain integro-differential equations of motion for a general viscoelastic body. A perturbation method is then used to solve the corresponding eigenvalue problem. To model the time-varying modulus G, a continuous decay distribution function γ is defined such that

$$G(t) = \int_0^\infty E_\infty \gamma(\theta) e^{-\theta t} d\theta \tag{4.5}$$

It is concluded that this decay distribution function needs to be established for various materials.

A constitutive model similar to the standard model is utilized by Bagley and Torvik [76], in which the differential operators consist of fractional derivatives. Their general constitutive model is written as

$$\sigma + \sum_{m=1}^{M} b_m D^{\beta_m} \{\sigma\} = E_\infty \varepsilon + \sum_{n=1}^{N} E_n D^{\alpha_n} \{\varepsilon\} \tag{4.6}$$

where $D^{\beta_m}\{.\}$ and $D^{\alpha_n}\{.\}$ are fractional derivative operators and b_m, β_m, E_n, and α_n are constant parameters. Experimental observations have indicated that many viscoelastic materials can be modeled by retaining only the first terms of the series, resulting in the five-parameter model

$$\sigma + b \frac{d^\beta \sigma}{dt^\beta} = E_\infty \varepsilon + E_1 \frac{d^\alpha \varepsilon}{dt^\alpha} \tag{4.7}$$

where β and α are fractions. Bagley and Torvik utilize the constitutive model of Eq.(4.7) to solve the eigenproblem associated with a viscoelastic structure in the Laplace domain. The problem associated with this model is that the eigensolution requires determination of a common denominator for β and α, which leads to a potentially very high order system to solve.

Golla and Hughes [77] also use the constitutive model given in Eq.(4.4), which can be written in the Laplace domain as

$$\sigma(s) = E_\infty \varepsilon(s) + s\, G(s)\, \varepsilon(s) \tag{4.8a}$$

$$= [E_\infty + g(s)]\, \varepsilon(s) \tag{4.8b}$$

The Laplace function g(s) is chosen to be a rational function of the form

$$g(s) = \sum_{i=1}^{n} \frac{a_i\, s}{s + b_i} \tag{4.9}$$

In obtaining discretized equations of motion for a viscoelastic structure, Golla and Hughes first formulate the equations of motion in the Laplace domain and then obtain a corresponding time-domain realization.

A very attractive method of modeling viscoelastic structures with slowly varying properties, as well as structures exhibiting slow stiffness degradation, is to write the constitutive relation in the form (for a one-dimensional stress state)

$$\sigma(t) = E_{\infty}\, [1 - \alpha(t)]\, \varepsilon(t) \tag{4.10}$$

where α is a general time- and space-dependent parameter referred to as the internal state variable [78-80]. It can be observed from the general one-dimensional constitutive model of Eq.(4.4) that if G(t) is a slowly varying parameter it can be approximated as a constant over relatively short periods of time, resulting in the constitutive law

$$\sigma(t) = [E_{\infty} + G(t)]\, \varepsilon(t) \tag{4.11}$$

Therefore, a viscoelastic constitutive model with slowly varying parameters can be described by the form of Eq.(4.10). In References

[78] through [80] it is shown that the constitutive model of Eq.(4.10) can be used to represent degradation of stiffness properties in composite laminates due to matrix cracking, interlaminar fracture, fiber breakage, and fiber/matrix debonding. Kalyanasundaram, et. al. [80] show the effects of the slowly varying internal state variable on the natural frequencies and mode shapes of a truss structure. As a model of the internal state variable, the following power law is chosen

$$\alpha(t) = k \left(\frac{\sigma(t)}{\sigma_{max}}\right)^{n} \tag{4.12}$$

where σ_{max} is the maximum stress in the structure and k and n are slowly varying parameters. For a maximum loss of 25% in axial stiffness (in the highest stressed members), it is shown that an 8% reduction in the value of the first three natural frequencies is obtained.

All of the methods described above require knowledge of the parameters of the relaxation modulus, either in the time-domain or in a transformed domain (Laplace domain or frequency domain). In the following section, a simple method of estimating the relaxation modulus is developed by assuming time-localized linear elastic behavior.

4.2 Quasi-Elastic Identification of the Relaxation Modulus

In this section a simple, practical identification technique is developed for materials whose relaxation modulus consists of a series of decay exponentials, as given by Eq.(4.2). Assuming the relaxation modulus varies slowly with time, the identification proceeds as

follows. Determination of the mass, viscous damping, and stiffness matrices is obtained from measured complex eigenvalues and frequency response functions at an early time in the life of the material (t_1) . At a considerable time later (t_2) the identification process is repeated with a new set of measured eigenvalues and frequency response functions. Repeating this process for a number of times throughout the life of the material allows for an estimate of the variation in the relaxation modulus E(t) using a simple curve fitting method.

For a viscoelastic material modeled with a Maxwell chain, the time dependence of the relaxation modulus can be taken as a series of exponentials

$$E(t) = E_\infty + \sum_{r=1}^{N} E_r e^{-p_r t} \qquad p_r \geq 0 \tag{4.13}$$

which implies the stress-strain relation can be represented as an array of springs and dashpots. According to Eq.(4.13), the relaxation modulus will initiate at some value $E(0) = E_0$ and asymptotically converge to a final value $E(\infty) = E_\infty$. If an initial estimate of the parameters are available, a nonlinear least-squares estimate of the parameters can be obtained from the locally identified values of the stiffness. If an initial estimate is not available, a linear least-squares curve fit of the identified stiffness variation can be obtained by choosing a model which exhibits the convergence properties of Eq.(4.13).

A very common model used to fit relaxation moduli over a very broad time scale is the modified power law [81]

$$E(t) = E_\infty + \frac{E_0 - E_\infty}{(1 + at)^n} \tag{4.14}$$

where E_0 , E_∞ , n, and a are non-negative constants and $0 \le n < 1$. Although the number of parameters is small, a curve fit with this model would require a nonlinear least-squares approach with initial estimates of the parameters. A more attractive method is to simply estimate the modulus parameters of Eq.(4.13) for a given set of prescribed relaxation time constants p_r (r=1,2,...,N) . By choosing the time constants to be equally spaced by no more than one decade (one order of magnitude), Schapery [82] shows that a smooth, accurate curve fit can be easily accomplished. A linear least-squares curve fit can be formulated as

$$\begin{Bmatrix} E(t_1) \\ E(t_2) \\ \vdots \\ E(t_M) \end{Bmatrix} = \begin{bmatrix} 1 & L_{11} & L_{21} & \cdots & L_{N1} \\ 1 & L_{12} & L_{22} & \cdots & L_{N2} \\ \vdots & \vdots & & \ddots & \\ 1 & L_{1M} & L_{2M} & \cdots & L_{NM} \end{bmatrix} \begin{Bmatrix} E_\infty \\ E_1 \\ \vdots \\ E_N \end{Bmatrix} \tag{4.15a}$$

where $$L_{jk} = e^{-p_j t_k} \tag{4.15b}$$

If the complex frequency domain modulus is desired, the Fourier transform of the hereditary integral of Eq.(4.3) can be used. The frequency domain constitutive equation becomes

$$\sigma(i\omega) = i\omega E(i\omega)\, \varepsilon(i\omega) = \hat{E}(i\omega)\, \varepsilon(i\omega) \tag{4.16}$$

where $\hat{E}(i\omega)$ is the complex modulus [69,72]. For a relaxation modulus that obeys Eq.(4.13), the complex modulus is written as

$$\hat{E}(i\omega) = E_\infty + \sum_{r=1}^{N} \frac{i\omega E_r}{i\omega + p_r} \tag{4.17a}$$

$$= E'(\omega)\,[1 + i\eta(\omega)] \tag{4.17b}$$

where $E'(\omega)$ is the storage modulus and $\eta(\omega)$ is the loss factor.

Example 4.1 Identification of a Viscoelastic Rotating Blade

The relaxation stiffness for the rotating blade shown in Figure 4.2 is identified using the quasi-elastic approach developed in the foregoing section. The blade is manufactured from a viscoelastic material whose model is representative of a five-parameter solid. To cast the model in terms of mass and stiffness submatrices, the following element groups are chosen:

Group I Global mass matrix

Group II Stiffness contribution from the flexibility of the blade

group III Stiffness contribution from the rotation of the blade

The determination of the stiffness relaxation proceeds as follows: (i) the identification of the mass and stiffness properties of the structure at a starting time (t = 0) is obtained from an initial approximation of the model using measurements of the first three natural frequencies and the frequency response function at point A, (ii) at succeeding time intervals, the identification is repeated with a new set of measurements and an initial model obtained from the previous time step, and (iii) a simple curve fit of the resulting stiffness variation is obtained by judiciously choosing a set of relaxation time constants and determining the corresponding moduli using Eq.(4.15). The true relaxation modulus for the material is assumed to have the form

$$EI(t) = 10{,}000 + 15{,}000\, e^{-2.3 \times 10^{-7} t} + 5000\, e^{-5.1 \times 10^{-6} t} \quad (4.18)$$

and the model used to curve fit the identified variation in the modulus is

$$EI(t) = EI_{\infty} + \sum_{r=1}^{6} EI_r\, e^{[-1 \times 10^{-5} / 5^{(r-1)}]\, t} \quad (4.19)$$

The resulting time and frequency variations in the identified relaxation stiffness (EI(t)) are presented in Figures 4.3 and 4.4, respectively. It is observed that, although the time variation in the relaxation modulus can be very accurately predicted, the Fourier transform of the identified modulus of Eq.(4.19) yields only a reasonable approximation of the frequency variation. A more accurate approximation of the frequency variation in the modulus may be obtained by curve fitting measurements of the relaxation modulus in the frequency domain itself. Of course, these results would then only yield a "reasonable approximation" of the time variation in the relaxation modulus.

It is evident that prescription of a parametric form such as Eq.(4.19) is a key ingredient for identification of viscoelastic materials with time-varying properties. Such insight can only be obtained by more fundamental constitutive modeling and/or appropriate material property characterization experiments. On the other hand, it is observed that a sequence of quasi-elastic identifications of effective elastic constants provides an excellent approach for determining the macroscopic effects of viscoelastic members on the slow variation in overall structural response characteristics.

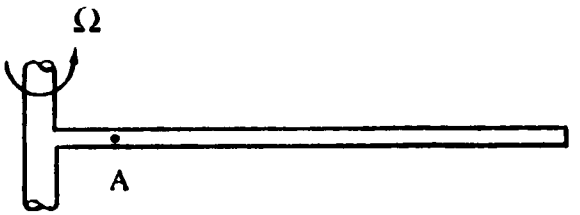

Parameters

$EI(t)=(10{,}000 + 15{,}000e^{-2.3\times10^{-7}t} + 5{,}000e^{-5.1\times10^{-6}t})$ lb·in^2

ρ = 0.0009 slug/in Length = 100 in

Ω = 5 rad/sec

Figure 4.2 Viscoelastic Rotating Helicopter Blade

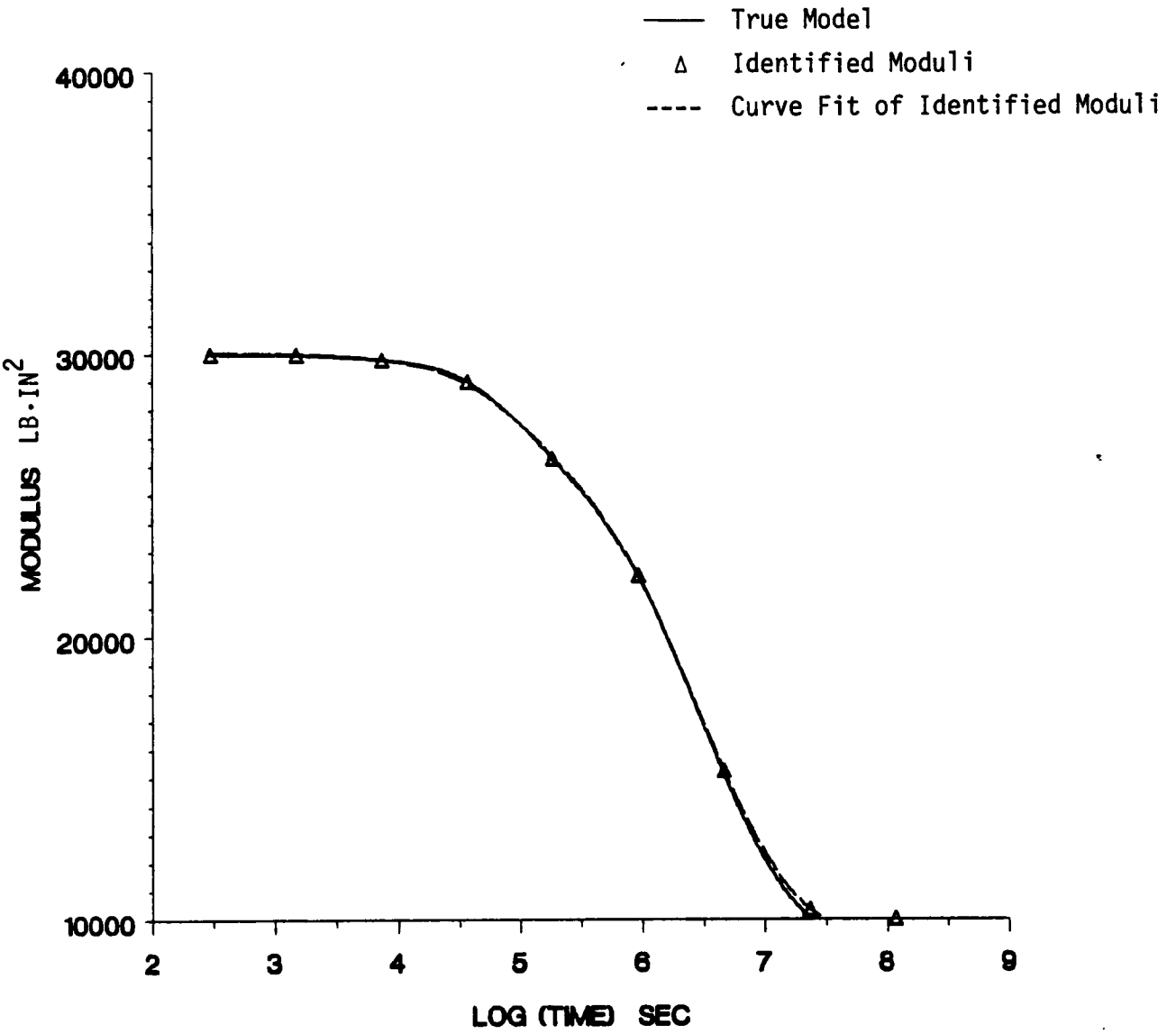

Figure 4.3 Identified Relaxation Modulus

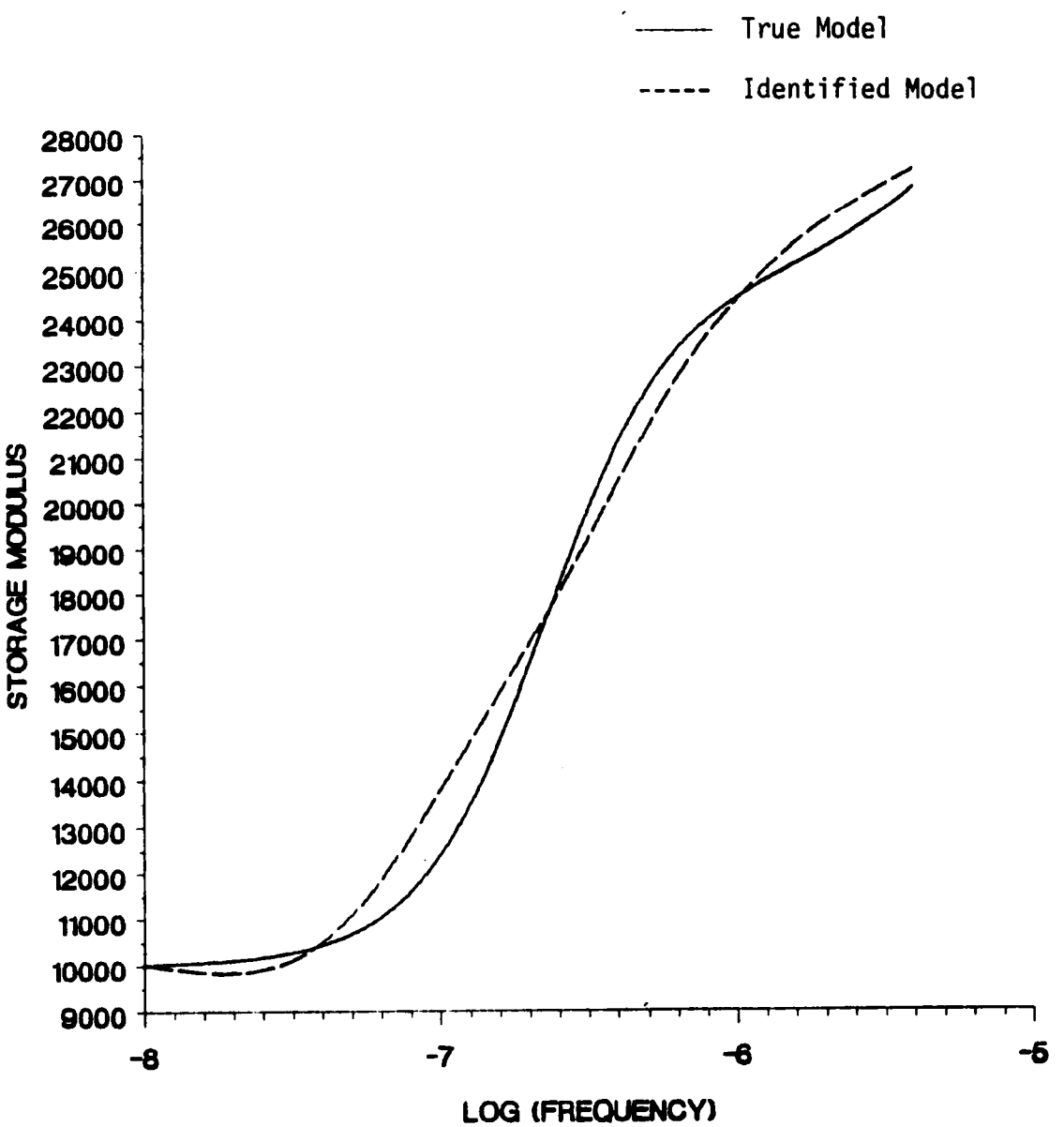

Figure 4.4a Identified Storage Modulus

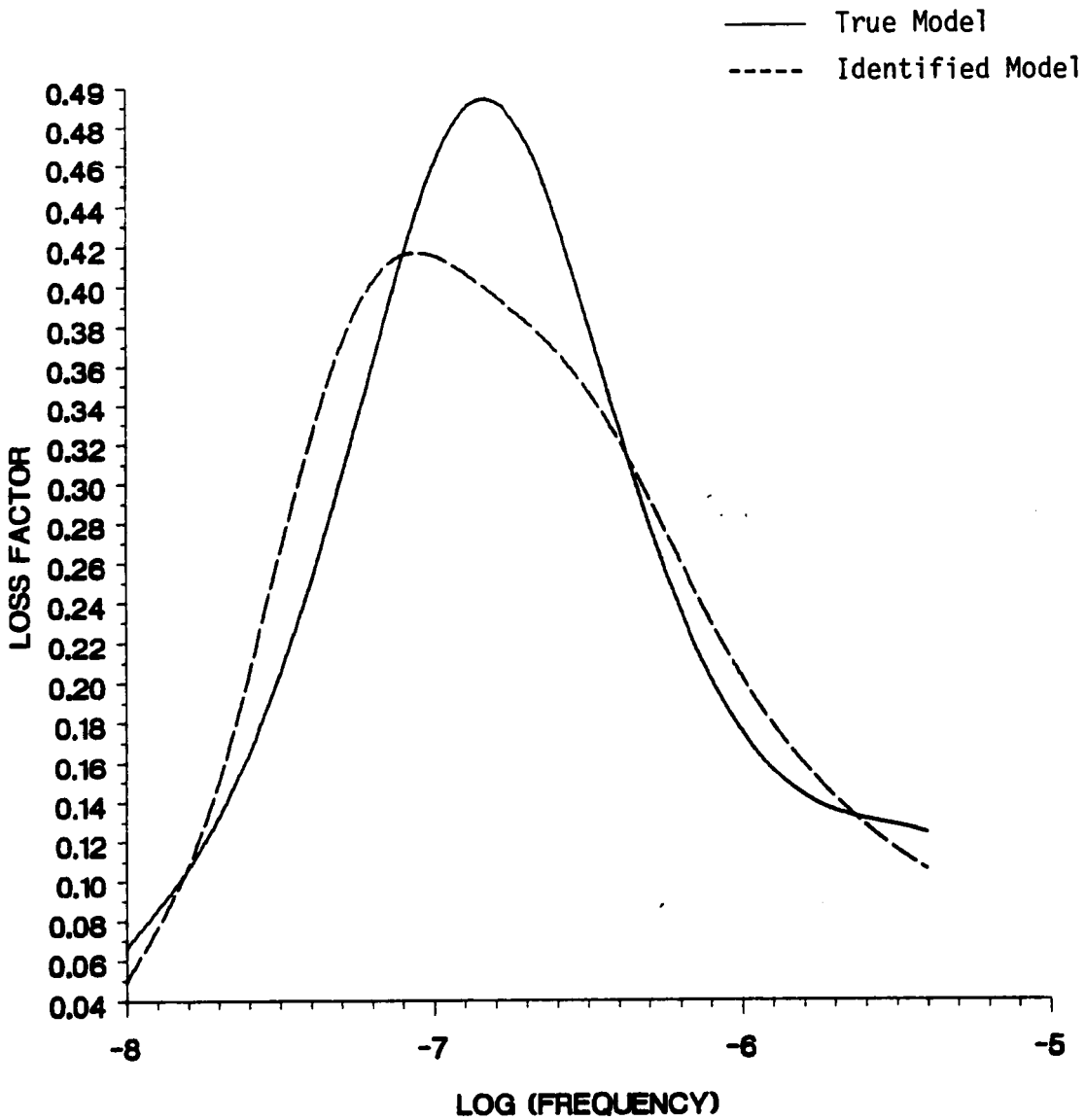

Figure 4.4b Identified Loss Factor

5. CONCLUSIONS

The accurate knowledge of the parameters of a structural model is of fundamental importance in the design and analysis of flexible structures. In this dissertation, a novel linear structural model identification method has been presented for improving the mass, damping, and stiffness matrices of an initial structural model in the event that the theoretical and experimental results are not in agreement. As a pre-processor for the new identification method, a modal identification technique is required to determine a set of measured eigenvalues and frequency response elements from time-domain records. The identification method, as developed in Chapter 3 for elastic structures, can be summarized as follows:

For undamped or lightly damped structures,

1. A set of modal normalization factors are identified from a small set of frequency response elements, measured throughout the frequency range of interest, and the imaginary components of a set of measured eigenvalues using the configuration-space spectral decomposition of the frequency response matrix. These modal factors normalize the initial mode shapes (obtained from available measurements or from the initial structural model) with respect to the true (unknown) mass matrix.
2. The initial mass, damping, and stiffness matrices are expanded into prescribed submatrices, each of which can represent a single finite element or a group of elements having the same assumed geometry,

material properties, boundary conditions, and modeling assumptions.

3. A set of submatrix scale factors, corresponding to each mass and stiffness submatrix, is identified using the orthonormality properties imposed on the mode shapes and the imaginary components of the measured eigenvalues.
4. In the presence of light damping, matrix perturbation theory is utilized to determine the damping submatrix scale factors from the real components of the measured eigenvalues.

For significantly damped structures,

1. A set of modal normalization factors are identified from measurements of a set of complex frequency response elements and eigenvalues using the state-space spectral decomposition of the frequency response function. These modal factors normalize the complex eigenvectors with respect to the true A matrix in $A\dot{z} + B z = f$.
2. The initial mass, damping, and stiffness matrices are expanded into prescribed submatrices.
3. A set of submatrix scale factors, corresponding to each submatrix, is identified from the orthonormality conditions imposed on the complex eigenvectors.

The interesting examples developed in the dissertation demonstrate the applicability, flexibility, and potential of the new method. The most important advantages are summarized as follows:

i) The incorporation of measured frequency response elements provides a unique identification of the structural model without the need to constrain any parameters to their initial estimates.

ii) All least-squares formulations are linear. The only requirement imposed on the initial estimate of the structural model is that the initial mode shapes represent a reasonable approximation of the true mode shapes.

iii) The consistency of the original structural model is maintained in the sense that no unmodeled coupling is introduced as a consequence of the identification process.

iv) Use of submatrix scale factors limits the identification to a relatively small set of parameters and, in many cases, allows the engineer to judiciously choose subproblems to identify.

v) For lightly damped structures, the identification can be performed in the (n dimensional) configuration space without the need to solve the (2n dimensional) state space eigenproblem.

vi) For lightly damped structures, the original estimate of the damping matrix need only represent the true matrix in the coupling of the elements (the initial numerical values can be off by orders of magnitude).

vii) The identification method can be easily incorporated into a substructure synthesis package for identification of each substructure model using a set of measurements obtained from the response of the assembled global structure.

For a structure containing viscoelastic members, a simple, practical approach for identification of a slowly-varying relaxation modulus is developed in Chapter 4. By assuming time-localized elastic behavior, the relaxation modulus can be very accurately determined from a series of identification tests performed at various times throughout the history of the response. This method is also attractive for identifying stiffness degradation in a structure.

In closing, some questions which should be considered as topics for further research and investigation are:

i) In application of the identification method to an actual structure, what effects will "real" modeling errors (such as unmodeled small nonlinearities and imperfect boundary conditions) and measurement noise have on the reliability of the method? As described in Section 3.2.a, to formally "test" the identified model requires a statistical analysis in which the free- and forced-response measurement errors and the initial modeling errors are propagated (in the form of covariance matrices) into the parameter estimation process. If these covariances can be approximated quantitatively, perhaps a refinement of the initial finite element model can be performed (i.e. by improving or increasing the element distributions, improving modeled boundary constraints, etc.) so that the identification process yields a statistically significant model.

ii) Can the identification method be extended to identify weakly nonlinear (material and/or geometrical) structural models of systems known to possess such nonlinearities? Perhaps a perturbation approach or a locally linear approach analogous to that developed for

viscoelastic structures can be developed for a certain class of nonlinearities.

iii) Can "equivalent" damping and stiffness matrices be identified for structures exhibiting viscoelastic response characteristics? It is shown in Chapter 4 that a slowly varying relaxation modulus can be accurately identified. However, since this approach is not feasible for structures exhibiting "short" viscoelastic time responses, perhaps effective viscoelastic damping and stiffness matrices can be determined to adequately predict the response of these structures.

REFERENCES

1. Astrom, K.J. and P. Eykhoff, "System Identification - A Survey," Automatica, Vol. 7, pp. 123-162, 1971.

2. Bekey, G., "System Identification: An Introduction and a Survey," Simulation, Vol. 15, pp.151-166, 1970.

3. Ibanez, P., "Review of Analytical and Experimental Techniques for Improving Structural Dynamic Models," Welding Research Council Bulletin, No. 249, June 1979.

4. Sage, A.P., "System Identification - History, Methodology, Future Prospects," System Identification of Vibrating Structures, Annual Winter Meeting of the ASME, 1972.

5. Collins, J.D., Young, J.P., and L.A. Kiefling, "Methods and Applications of System Identification in Shock and Vibration," System Identification of Vibrating Structures, Annual Winter Meeting of the ASME, 1972.

6. Hart, G.C. and J.P. Yao, "System Identification in Structural Dynamics," ASCE Journal of Engineering Mechanics Div., Vol. 103, No. EM6, Dec. 1977.

7. Berman, A., "Determining Structural Parameters from Dynamic Testing," Shock and Vibration Digest, Vol. 7, Jan. 1975.

8. Flannelly, W.G. and A. Berman, "The State of the Art of System Identification of Aerospace Structures," System Identification of Vibrating Structures, Annual Winter Meeting of the ASME, 1972.

9. Junkins, J.L., Optimal Estimation of Dynamical Systems, Sijthoff and Noordhoff Alpen aan den Rijn, The Netherlands/Rockville, Maryland, U.S.A., 1978.

10. Broemeling, L.D., Bayesian Analysis of Linear Models, Marcel Dekker, Inc., New York, 1985.

11. Deutsch, R., Estimation Theory, Prentice-Hall, Inc., Englewood Cliffs, N.J., 1965.

12. Isenberg, J., "Progressing from Least Squares to Bayesian Estimation," ASME Winter Annual Meeting, New York City, New York, December, 1979.

13. Hendricks, S.L., Hayes, S.M., and J.L. Junkins, "Structural Parameter Identification for Flexible Spacecraft," AIAA Paper No. 84-0060, Presented at the AIAA 22nd Aerospace Sciences Meeting, Jan. 9-12, 1984.

14. Creamer, N.G. and S.L. Hendricks, "Structural Parameter Identification Using Modal Response Data," Proceedings of the Fifth VPI & SU/AIAA Symposium on Dynamics and Control of Large Flexible Spacecraft, VPI & SU, Blacksburg, VA, L. Meirovitch, ed., June, 1985.

15. Caravani, P., Watson M.L., and W.T. Thomson, "Recursive Least Squares Time Domain Identification of Structural Parameters," J. of Applied Mech., Vol. 44, pp. 135-140, 1977.

16. Chen, J.C. and J.A. Garba, "Analytical Model Improvement Using Modal Test Results," AIAA Journal, Vol. 18, No. 6, June, 1980, pp. 684-690.

17. Collins, J.D., Hart, G.C., Hasselman, T.K., and B. Kennedy, "Statistical Identification of Structures," AIAA Journal, Vol. 12, No. 2, February, 1974, pp. 185-190.

18. Dobbs, M.W. and R.B. Nelson, "Parameter Identification of Large Structural Models - Concept and Reality," ASME Winter Annual Meeting, Boston, Massachusetts, November, 1983.

19. Beliveau, J., "Identification of Viscous Damping in Structures From Modal Information," J. Applied Mech., Vol. 43, pp. 335-339, June, 1976.

20. Hasselman, T.K. and L. Johnson, "Validation and Verification of Rail Vehicle Models," ASME Paper No. 79-WA/DSC-8, Presented at the ASME Winter Annual Meeting, New York, New York, Dec. 2-7, 1979.

21. Fries, R.H. and N.K. Cooperrider, "Bayesian Estimation of Transit Rail Vehicle Parameters," Journal of Dynamic Systems, Measurements, and Control, June 1985, Vol. 107, pp. 151-158.

22. Hasselman, T.K. and J.D. Chrostowski, "Parameter Estimation For Large Space Structures," Proceedings of the Session Sponsored by the ST Div./ASCE/Spring Convention, Denver, CO, May 1, 1985.

23. Lee, L.T. and T.K. Hasselman, "Dynamic Model Verification of Large Structural Systems," Paper No. 781047 presented at the SAE Aerospace Meeting, San Diego, CA, Nov. 27-30, 1978.

24. Chrostowski, J.D., Evensen, D.A., and Hasselman, T.K., "Model Verification of Mixed Dynamic Systems," ASME Journal of Mechanical Design, Vol. 100, April 1978.

25. Hasselman, T.K., "A Perspective on Dynamic Model Verification," ASME Winter Annual Meeting, Boston, Massachusetts, November, 1983.

26. Hart, G.C. and D.R. Martinez, "Improving Analytical Dynamic Models Using Frequency Response Data - Application," Paper 82-0637-CP, AIAA/ASME/ASCE/AHS 23rd SDM Conference, New Orleans, May 10-12, 1982.

27. Martinez, D.R., "Estimation Theory Applied to Improving Dynamic Structural Models," Sandia Report No. SAND82-0572, Sandia National Laboratories, Albuquerque, NM, Nov. 1984.

28. Noor, A.K. and C.M. Anderson, "Analysis of Beam-Like Lattice Trusses," Comp. Meth. Appl. Mech. Engrg., Vol. 20, 1979, pp. 53-70.

29. Chen, C.C. and C.T. Sun, "Transient Analysis of Large Frame Structures by Simple Models," Proceedings of Symposium on Engineering Science and Mechanics, National Cheng Kung University/American Astronautical Society, Dec. 28-31, 1981.

30. Sun, C.T., Kim, B.J., and Bogdanoff, J.L., "On the Derivation of Equivalent Simple Models for Beam- and Plate-Like Structures in Dynamic Analysis,"Proceedings AIAA Specialists Conference, Atlanta, Georgia, April 6-8, 1981, pp. 523-532.

31. Juang, J.N. and C.T. Sun, "System Identification of Large Flexible Structures by Using Simple Continuum Models," J. of Astronautical Sciences, Vol. 31, pp. 77-98, 1983.

32. Sun, C.T. and J.N. Juang, "Parameter Estimation in Truss Beams Using Timoshenko Beam Models With Damping," Workshop on Applications of Distributed System Theory to the Control of Large Space Structures, JPL Publication 83-46, July 1983.

33. White, C.W. and B.D. Maytum, "Eigensolution Sensitivity to Parametric Model Perturbations," Shock and Vibration Bulletin, Bulletin 46, part 5, Aug., 1976, pp. 123-133.

34. Berman, A. and W.G. Flannely, "Theory of Incomplete Models of Dynamic Structures," AIAA Journal, Vol. 9, No. 8, August, 1971, pp. 1481-1487.

35. Berman, A. and E.J. Nagy, "Improvement of Large Analytical Model Using Test Data," AIAA Journal, Vol. 21, No. 8, August, 1983, pp. 1168-1173.

36. Berman, A., "Mass Matrix Correction Using an Incomplete Set of Measured Modes," AIAA Journal, Vol. 17, No. 10, October, 1979, pp. 1147-1148.

37. Wei, F.S., "Stiffness Matrix Corrections from Incomplete Test Data," AIAA Journal, Vol. 18, Oct. 1980, pp. 1274.

38. Chen, J.C., Kuo, C.P. and J.A. Garba, "Direct Structural Parameter Identification by Modal Test Results," Presented at the AIAA/ASME/ASCE/AAS SDM Conference, May 2-4, 1983.

39. Potter, R. and M. Richardson, "Mass, Stiffness, and Damping Matrices from Measured Modal Parameters," ISA Conference and Exhibit, New York, Oct. 1974.

40. Rajaram, S., "Identification of Vibration Parameters of Flexible Structures", Doctoral Dissertation, Virginia Polytechnic Institute and State University, Virginia, May, 1984.

41. Rajaram, S. and J.L. Junkins, "Identification of Vibrating Flexible Structures," AIAA Journal of Guidance, Control, and Dynamics, Vol. 8, No. 4, pp. 463-470, July-August, 1985.

42. Hendricks, S.L., Rajaram, S., Kamat, M.P., and J.L. Junkins, "Identification of Large Flexible Structures Mass/Stiffness and Damping From On-Orbit Experiments," AIAA Journal of Guidance, Control, and Dynamics, Vol. 7, No. 2, pp. 244-245, March-April, 1984.

43. Reddy, J.N., An Introduction to the Finite Element Method, McGraw-Hill, New York, 1984.

44. Ewins, D.J., Modal Testing: Theory and Practice, Research Studies Press Ltd., England, 1984.

45. Newland, D.E., Random Vibrations and Spectral Analysis, Longman Group Ltd, London, 1975.

46. Ramsey, K.A., "Effective Measurements for Structural Dynamics Testing - Part I," Sound and Vibration, Nov. 1975.

47. Ramsey, K.A., "Effective Measurements for Structural Dynamics Testing - Part II," Sound and Vibration, April 1976.

48. Mitchell, L.D., "Improved Methods for the Fast Fourier Transform (FFT) Calculation of the Frequency Response Function," Trans. ASME, Journal of Mach. Design, Vol. 104, pp. 277-279, April 1982.

49. Mitchell, L.D., "Signal Processing and the Fast Fourier Transform (FFT) Analyzer - A Survey," Presented at the SEM Spring Conference on Experimental Mechanics, Las Vegas, June 9-14, 1985.

50. Ewins, D.J. and P.T. Gleeson, "A Method for Modal Identification of Lightly Damped Structures," Journal of Sound and Vibration, 84(1), 1982, pp. 57-79.

51. Gaukroger, D.R., K.H. Heron, and C.W. Skingle, "The Processing of Response Data to Obtain Modal Frequencies and Damping Ratios," Journal of Sound and Vibration, Vol. 35, pp. 559-571, 1974.

52. Richardson, M. and R. Potter, "Identification of the Modal Properties of an Elastic Structure from Measured Transfer Function Data," 20th ISA, Albuquerque, May 1974.

53. Richardson, M., and J. Kniskern, "Identifying Modes of Large Structures of an Elastic Structure from Measured Transfer Function Data," ISA/ASI 74250, pp. 239-246, 1974.

54. Ibrahim, S.R. and E.C. Mikulcik, "A Time Domain Modal Vibration Test Technique," Shock and Vibration Bulletin, Bulletin 43, Part 4, 1973, pp. 21-37.

55. Ibrahim, S.R. and E.C. Mikulcik, "The Experimental Determination of Vibration Parameters from Time Responses," Shock and Vibration Bulletin, Part 5, pp. 187-195, 1976.

56. Ibrahim, S.R. and E.C. Mikulcik, "A Method for the Direct Identification of Vibration Parameters from the Free Response," Shock and Vibration Bulletin, No. 43, pp. 21-37, 1973.

57. Juang, J.N. and R.S. Pappa, "An Eigensystem Realization Algorithm for Modal Parameter Identification and Model Reduction," Journal of Guidance, Control, and Dynamics, Vol. 8, No. 5, Sept-Oct, 1985.

58. Pappa, R.S. and J.N. Juang, "Galileo Spacecraft Modal Identification Using an Eigensystem Realization Algorithm," The Journal of the Astronautical Sciences, Vol. 33, No. 1, Jan-Mar, 1985.

59. Juang, J.N. and R.S. Pappa, "Effects of Noise on ERA-Identified Modal Parameters," AAS/AIAA Astrodynamics Specialist Conference, Vail, CO, August 12-15, 1985.

60. Klema, V.C. and A.J. Laub, "The Singular Value Decomposition: Its Computation and Some Applications," IEEE Transactions on Automatic Control, Vol. AC-25, No. 2, April 1980.

61. Paz, M., "Dynamic Condensation," AIAA Journal, Vol. 22, No. 5, May 1985.

62. Paz, M., Structural Dynamics - Theory and Computation, Van Nostrand Reinhold Co., New York, 1985.

63. Hurty, W.C., "Dynamic Analysis of Structural Systems Using Component Modes," AIAA Journal, Vol. 3, 1965.

64. Craig, R.R. and M.C. Bampton, "Coupling of Substructures for Dynamic Analysis," AIAA Journal, Vol. 6, 1968.

65. Craig, R.R., Structural Dynamics - An Introduction to Computer Methods, John Wiley and Sons, New York, 1981.

66. Caughey, T.K. and C.J. Goh, "Vibration Suppression in Large Space Structures," NASA-CR-173119, Proceedings of the Workshop on Applications of Distributed System Theory to the Control of Large Space Structures, July 1, 1983.

67. Rew, D.W. and J.L. Junkins, "Multi-Criterion Approaches to Optimization of Linear Regulators," AIAA Paper 86-2198-CP, Presented at the AIAA Guidance, Navigation, and Control Conference, Williamsburg, VA, August, 1986, to appear in the Journal of Astronautical Sciences.

68. Meirovitch, L., Computational Methods in Structural Dynamics, Sijthoff & Noordhoff, The Netherlands, 1980.

69. Flugge, W., Viscoelasticity, Springer-Verlag, New York, 1975.

70. Holzlohner, U., "A Finite Element Analysis for Time-Dependent Problems," Int. Jour. for Num. Meth. in Eng., Vol. 8, pp. 55-69, 1974.

71. Hendricks, S.L., "The Effect of Viscoelasticity on the Vibration of a Rotor," Journal of Applied Mechanics, Vol. 53, pp. 412-416, June 1986.

72. Christensen, R.M., Theory of Viscoelasticity - An Introduction, Academic Press, New York, 1971.

73. Yamada, Y., Takabatake, H., and T. Sato, "Effect of Time-Dependent Material Properties on Dynamic Response," Int. Jour. for Num. Meth. in Eng., Vol. 8, pp. 403-414, 1974.

74. Pinnamaneni, M. and D.R. Mokadam, "A Methodology for the Dynamic Viscoelastic Analysis of Solid Propellant Motors," Presented at the AIAA/ASME/ASCE/AHS 27th SDM Conference, San Antonio, 1986.

75. Buhariwala, K.J., "Dynamics of Viscoelastic Structures," Doctoral Dissertation, University of Toronto, Toronto, 1984.

76. Bagley, R.L. and P.J. Torvik, "Fractional Calculus - A Different Approach to the Analysis of Viscoelastically Damped Structures," Presented at the AIAA/ASME/ASCE/AHS 22nd SDM Conference, Atlanta, April 6-8, 1981.

77. Golla, D.F. and P.C. Hughes, "Dynamics of Viscoelastic Structures - A Time-Domain Finite Element Formulation," Journal of Applied Mechanics, Vol. 52, Dec. 1985.

78. Allen, D.H., Groves, S.E., Schapery, R.A. and C.E. Harris, "A Thermomechanical Constitutive Theory for Elastic Composites with Distributed Damage - Part I: Theoretical Development," Mechanics and Materials Center, Texas A&M Univ., College Station, TX, Report MM 5023-85-16, Sept. 1985.

79. Groves, S.E., Allen, D.H., Harris, C.E., and S.E. Schapery, "A Thermomechanical Constitutive Theory for Elastic Composites with Distributed Damage - Part II: Application to Matrix Cracking in Laminated Composites," Mechanics and Materials Center, Texas A&M Univ., College Station, TX, Report MM 5023-85-15, Oct. 1985.

80. Kalyanasundaram, S., Lutz, J.D., Haisler, W.E., and D.H. Allen, "Effect of Degradation of Material Properties on the Dynamic Response of Large Space Structures," Presented at the AIAA/ASME/ASCE/AHS 26th SDM Conference, Orlando, FL, April 15-17, 1985.

81. Schapery, R.A., "Viscoelastic Behavior and Analysis of Composite Materials," Mechanics of Composite Materials - Volume 2, ed. G.P. Sendeckyj, Academic Press, New York, 1974.

82. Schapery, R.A., "A Simple Collocation Method for Fitting Viscoelastic Models to Experimental Data," Calif. Ins. of Tech., Report GALCIT SM 61-23A, 1961.

The vita has been removed from the scanned document